Synthesis, Characterization, and Transition-Metal Complexes of 3,4-Diazaphospholanes

Clark R. Landis,* Ryan C. Nelson, Wiechang Jin, and Amanda C. Bowman

Department of Chemistry, University of Wisconsin−Madison, 1101 University of Ave., Madison, Wisconsin 53706

Received October 24, 2005

The steric, electronic, and synthetic characteristics of 3,4-diazaphospholanes are reported. Crystallographic structures of free and metal-complexed 3,4-diazaphospholanes provide steric metrics (cone angle, solid angle, etc.). Diazaphospholanes span a wide range of sizes with cone angles varying from 135 to 188°. The electron-donating abilities of diazaphospholanes have been estimated using the carbonyl infrared stretching frequencies, ν(CO), of [*trans*-Rh(diazaphospholane)$_2$(CO)Cl] complexes. Frequencies for the CO stretches range from 1975 to 2011 cm^{-1}, thus indicating that 3,4-diazaphospholanes may be as electron rich as dialkylarylphosphines or as electron deficient as trialkyl phosphites. Reduction of *N*,*N*′-phthalamido-3,4-diazaphospholanes with BH_3·SMe_2 yields diazaphospholanes that not only are more electron rich but also show a reorientation of the phospholane substituents that may affect catalytic properties. Diazaphospholanes readily react with many Rh and Pd catalyst precursors to form complexes. Metal complexes of 3,4-diazaphospholanes exhibit reactivities different from those of common phosphine complexes, presumably due to the generally greater steric bulk and electron deficiency of 3,4-diazaphospholanes relative to phosphines. Cationic Rh(I) complexes of 3,4-diazaphospholanes abstract chloride ligands from chlorinated solvents to afford chloride-bridged dimers. The complex [(*rac*-**17**)Pd(Me)Cl] rearranges in solution—stereoselectively transferring methyl from palladium to phosphorus while simultaneously opening a diazaphospholane ring. Many of the 3,4-diazaphospholane−metal complexes have extremely close Cl···H−C(P)(N) contacts, suggesting Cl···H hydrogen bonding.

Introduction

Phosphine complexes of Rh and Pd enable a broad spectrum of catalytic transformations that form C−C, C−N, C−O, and C−H bonds.[1−3] Phospholanes constitute a particulary useful ligand family for creating new, efficient transition-metal catalysts. For example, Rh complexes of DuPHOS and its analogues exhibit high activities and enantioselectivities for a wide range of metal-catalyzed reactions.[4,5] Phosphine steric and electronic properties are powerful elements in controlling the reactivity and selectivity in phosphine-promoted metal-catalyzed reactions;[6−10] however, commonly used conditions for DuPHOS synthesis preclude placement of functional groups in the 2- and 5-positions of the phospholane ring that might be used to modulate the ligand steric and electronic properties.[4,5]

Recently, we reported that these limitations can be circumvented by introducing a set of chiral 3,4-diazaphospholanes based on a simple, acid-promoted reaction of azines (RHC═N−N═CHR) with a primary phosphine (Scheme 1, path A). This synthetic route provides C_2-symmetric bis-3,4-diazaphospholanes that bear structural similarity to DuPHOS and BPE.[11,12] With relative ease, this synthesis can be modified to make a range of phosphines having varying steric properties while also incorporating a variety of functional groups. Unfortunately, these phosphines can be unstable to retroaddition, particularly in the presence of transition metals. Functionalization of the 3,4-diazaphospholane nitrogen atoms as carboxamides (Scheme 1, path B) protects the phospholane against retroaddition, rigidifies

Scheme 1. General Synthesis of the 3,4-Diazaphospholanes

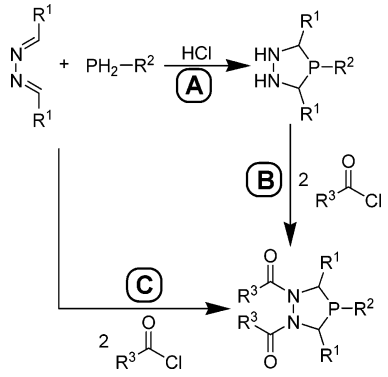

* To whom correspondence should be addressed. E-mail: landis@chem.wisc.edu.

(1) Beller, M., Bolm, C., Eds. *Transition Metals for Organic Synthesis*, 2nd ed.; Wiley-VCH: Weinheim, Germany, 2004; Vol. 1.
(2) Beller, M., Bolm, C., Eds. *Transition Metals for Organic Synthesis*, 2nd ed.; Wiley-VCH: Weinheim, Germany, 2004; Vol. 2.
(3) Müller, T. E.; Beller, M. *Chem. Rev.* **1998**, *98*, 675−703.
(4) Burk, M. J. *Acc. Chem. Res.* **2000**, *33*, 363−372.
(5) Clark, T.; Landis, C. *Tetrahedron: Asymmetry* **2004**, *15*, 2123−2137.
(6) Tolman, C. A. *Chem. Rev.* **1977**, *77*, 313−348.
(7) van Leeuwen, P. W. N. M.; Kamer, P. C. J.; Reek, J. N. H.; Dierkes, P. *Chem. Rev.* **2000**, *100*, 2741−2769.
(8) Cooney, K. D.; Cundari, T. R.; Hoffman, N. W.; Pittard, K. A.; Temple, M. D.; Zhao, Y. *J. Am. Chem. Soc.* **2003**, *125*, 4318−4324.
(9) Joerg, S.; Drago, R. S.; Sales, J. *Organometallics* **1998**, *17*, 589−599.
(10) Wilson, M. R.; Liu, H.; Prock, A.; Giering, W. P. *Organometallics* **1993**, *12*, 2044−2050.
(11) Landis, C. R.; Jin, W.; Owen, J. S.; Clark, T. P. Preparation of diazaphosphacycles and their corresponding transition metal complexes as allylic alkylation catalysts and hydrogenation catalysts. PCT Int. Appl. WO 2003010174, 2003.
(12) Landis, C. R.; Jin, W.; Owen, J. S.; Clark, T. P. *Angew. Chem., Int. Ed.* **2001**, *40*, 3432−3434.

10.1021/om050922g CCC: $33.50
Publication on Web 02/08/2006

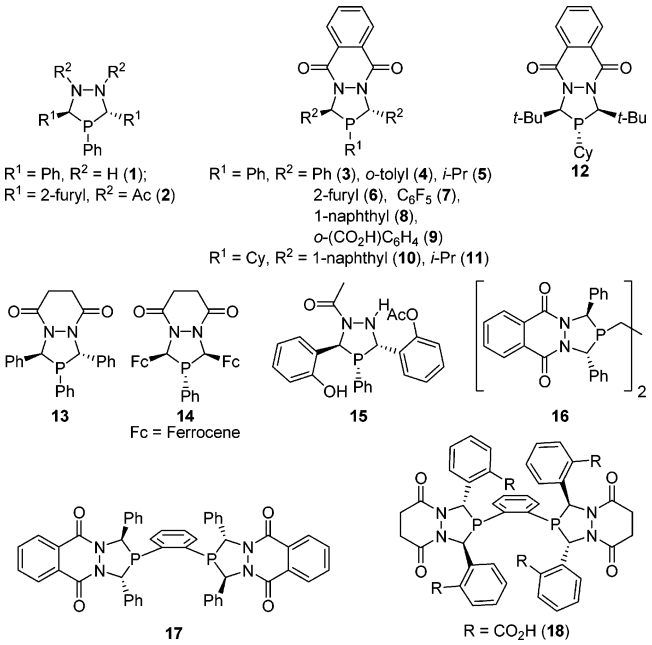

Figure 1. Selection of 3,4-diazaphospholanes synthesized to date.

the five-membered ring, and imparts considerable air stability to the phosphines, most of which can be handled and purified in air for several hours. Such N,N′ derivatization can be accomplished either in two separate steps or as a one-pot, simultaneous reaction of azine, primary phosphine, and acid chloride (Scheme 1, path C). In many cases, the one-pot procedure effects higher yields and is generally more convenient. In general, this three-component cyclization procedure forms the *rac* diastereomer as the major product; recrystallization or flash chromatography removes any *meso* products. A small sample of phosphines that have been prepared by these techniques is outlined in Figure 1.

The carboxylic acid functionalized phosphines *rac*-**9** and *rac*-**18** are particularly useful. Although these phosphines have not proven to be catalytically effective, modification through amino acid coupling chemistry leads to a large variety of phosphines that are effective in catalytic applications.[13,14] Use of enantiomerically pure amines in the coupling reaction produces diastereomeric carboxamides that are separable by flash chromatography or HPLC. In the special case of *rac*-**9**, synthesis on a multigram scale followed by recrystallization with either enantiomer of methylbenzylamine affords both enantiomers of the phospholanes in >99% ee.[14] Screening of carboxamide-functionalized monophosphines as ligands in the Pd-catalyzed asymmetric allylic alkylation (AAA) reaction led to the development of several catalysts exhibiting high enantioselectivities for alkylation of both dimethyl- and diphenylallyl acetate.[14] Supported catalysts generated from attachment of monophosphines to polymer beads give AAA results identical with those for the homogeneous catalyst.[15] Carboxamides derived from *rac*-**18** demonstrate remarkably high activities and enantioselectivities in the asymmetric hydroformylation of a variety of terminal alkenes.[13] Many other 3,4-diazaphospholanes have been tested in catalytic hydrogenation and hydroformylation, with promising initial results.[16]

Owing to the impressive catalytic results obtained with the 3,4-diazaphospholanes, we set out to gain a broader understanding of the chemical and physical properties of these ligands. We describe the synthesis of 3,4-diazaphospholanes, some of which have not been previously reported, and new procedures for reducing the carboxamide groups to simple tertiary amines. The steric sizes of diazaphospholanes, as determined by solid angle measurements derived from crystallographic structures, follow the synthetic descriptions. The electronic properties of 3,4-diazaphospholanes have been probed by the CO stretching frequencies of [*trans*-Rh(3,4-diazaphospholane)$_2$(CO)Cl] complexes. The presentation of results concludes with a description of the synthesis and structural features of rhodium and palladium complexes containing 3,4-diazaphospholane ligands. Novel reactivity patterns of metal complexes of 3,4-diazaphospholane include chloride abstraction from chlorinated solvents and opening of the 3,4-diazaphospholane ring.

Results and Discussion

Synthesis of 3,4-Diazaphospholanes and Borane Reduction. Previous reports have described the synthesis of many of the 3,4-diazaphospholanes used in these experiments.[12,14] Mixing azine, primary phosphine, and phthaloyl chloride in THF provides the 3,4-diazaphospholanes *rac*-**8** and *rac*-**10** in moderate yields (*rac*-**8**, 42%; *rac*-**10**, 61%). Improved syntheses of *rac*-**5** and *rac*-**11** are outlined as follows. Isobutyraldehyde and hydrazine are combined in benzene solvent and refluxed with a Dean−Stark trap to remove water. Distillation of the crude product mixture affords the isopropyl azine in a yield (77%) superior to that of the published method.[17] Unfortunately, the one-pot synthesis (Scheme 1, path C) of *rac*-**5** and *rac*-**11** is not effective; a side reaction (eq 1) becomes competitive with

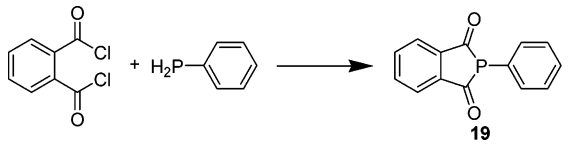

(1)

the diazaphospholane cyclization, leading to a large amount of the byproduct **19**.[18] To avoid the formation of **19**, the unprotected 3,4-diazaphospholanes first are synthesized by reaction of azine and phenylphosphine with 1 equiv of dry HCl. After workup, the unprotected phosphine can be reacted with phthaloyl dichloride in THF to give the final 3,4-diazaphospholane products in reasonable yields (*rac*-**5**, 73%; *rac*-**11**, 78%).

The bis-phosphine *rac*-**16** was made by the reaction of the previously reported *rac*-**20**[12] with phthaloyl dichloride in THF.

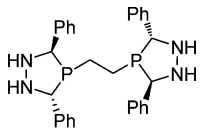

20

Synthesis of the bis-phosphine *rac*-**17** was refined by simply mixing 1,2-diphosphinobenzene and phenyl azine with phthaloyl dichloride in THF. Only the racemic bis-phosphine precipitated

(13) Clark, T. P.; Landis, C. R.; Freed, S. L.; Klosin, J.; Abboud, K. A. *J. Am. Chem. Soc.* **2005**, *127*, 5040−5042.

(14) Clark, T. P.; Landis, C. R. *J. Am. Chem. Soc.* **2003**, *125*, 11792−11793.

(15) Landis, C. R.; Clark, T. P. *Proc. Natl. Acad. Sci. U.S.A.* **2004**, *101*, 5428−5432.

(16) Landis, C. R.; Jin, W.; Owen, J. S.; Clark, T. P.; Nelson, R. C. Preparation of diazaphosphacycles and their use in transition metal catalyzed organic synthesis. PCT Int. Appl. WO 2005042546, 2005.

(17) Blackham, A. U.; Eatough, N. L. *J. Am. Chem. Soc.* **1962**, *84*, 2922−2930.

(18) Barron, A. R.; Hall, S. W.; Cowley, A. H. *J. Chem. Soc., Chem. Commun.* **1987**, 1753−1754.

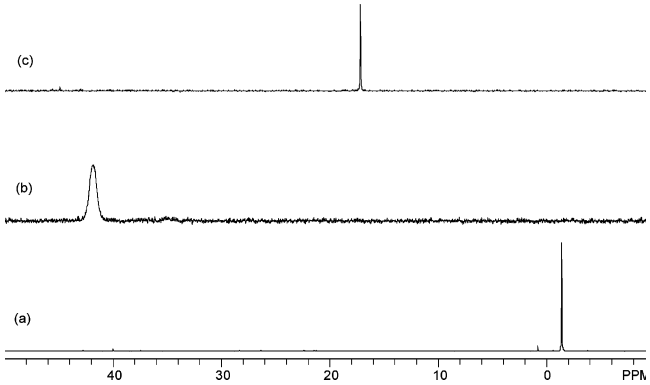

Figure 2. ^{31}P NMR spectra of (a) **3** in $CDCl_3$, (b) **21**·BH_3 in acetone-d_6, and (c) **21** in $CDCl_3$.

Scheme 2. Borane Reduction and Deprotection of the 3,4-Diazaphospholanes

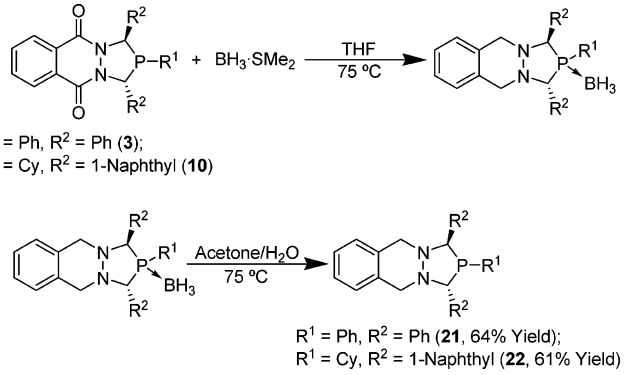

out of solution, and after the solid was rinsed and filtered, *rac*-**17** was isolated as an off-white solid. On the basis of the statistical probability for four stereocenters, the expected yield of *rac*-**17** is 13%; however, we consistently obtain around a 35% yield, which indicates a factor of 3 diastereomeric enrichment in the cyclization reaction.

The *N*,*N*′-acyl groups, which protect the 3,4-diazaphospholanes from retroaddition in the presence of transition metals, are particularly rigid and electron withdrawing; therefore, we sought a method to replace the acyls with alkyl protective groups to gauge the effect on the structure and properties of the 3,4-diazaphospholanes. Attempted N-alkylations of the unprotected diazaphospholanes (e.g., **1**) with alkyl halides either completely failed or resulted in alkylation at phosphorus. We then explored the possibility of reduction of the *N*,*N*′-diacyl-3,4-diazaphospholanes. Diacylhydrazine reductions using BH_3·SMe_2 have been reported to occur without rupture of the hydrazine bond,[19] suggesting that similar reduction of *N*,*N*′-diacyl-3,4-diazaphospholanes might be achieved.

Mixing a *N*,*N*′-diacyl-3,4-diazaphospholane, such as **3** or **10**, with excess BH_3·SMe_2 in THF followed by heating at 75 °C overnight in a sealed Schlenk flask yields the carboxamide reduction product (**21** or **22**) as the borane-protected phosphine. Refluxing the 3,4-diazaphospholane−borane adduct in slightly wet acetone overnight gives the unprotected phosphine in high purity and moderate yields (Scheme 2).

The reduction of *rac*-**3**, carried out in a sealed NMR tube, nicely illustrates the progress of borane reduction (Figure 2). The reduction of *rac*-**10** is similar; however, the ^{31}P NMR spectrum of the final product is much broader, presumably due to conformational dynamics.

(19) Feuer, H.; Brown, F., Jr. *J. Org. Chem.* **1970**, *35*, 1468−1471.

Diazaphospholane Steric Sizes. From the variety of methods available for the quantification of ligand sizes,[20−32] we chose to evaluate the 3,4-diazaphospholanes using solid-angle measurements.[20−25] If the metal is considered a point source of light, the solid angle (Ω) of a ligand is the normalized area of the shadow cast by the ligand on a sphere encompassing the entire complex. Solid angles have been applied not only toward the analysis of ligand steric sizes in coordination compounds but also to functional group sizes for some organic compounds.[33−37] The input data can come from either crystal structure data or modeling software, which broadens the available data pool. Furthermore, the calculations are extremely fast, enabling the analysis of large numbers of structures in a short time period.

To calculate the solid angles, we used a new program, developed by Drs. Ilia Guzei and Mark Wendt at the University of Wisconsin−Madison, called Solid-G, which is conceptually similar to the Steric program developed by Taverner and coworkers.[21,22] Solid-G utilizes a simple text file of orthogonal coordinates (obtained from the crystal structure or modeling program) to calculate the solid angle of all ligands bound to a specified atom. Solid-G not only calculates the solid angle for each ligand at its original metal−ligand bond distance but also translates each monodentate ligand to a set distance from the metal (2.28 Å) and recalculates a normalized steric value to facilitate comparison with other ligands. Multidentate ligands are normalized by moving the centroid of the ligated atoms to 2.28 Å and calculating the solid angle for the entire ligand. This method does not permit direct comparison of the steric sizes of multidentate ligands with monodentate ligands.

Solid angles are expressed in steradians, which range from 0 to 4π. For convenience, Solid-G converts the solid angle into two other useful quantities: area percent and cone angle. The area percent (%) refers to the percentage of the encompassing sphere that is occupied by the shadow of the ligand. The Solid-G cone angle (θ) is equivalent to reshaping the shadow of the ligand into a circle with the same area and measuring the cone angle of that circle, a method which generally leads to smaller values than the Tolman cone angles.

(20) White, D.; Coville, N. J. *Adv. Organomet. Chem.* **1994**, *36*, 95−158.
(21) Taverner, B. C.; Smith, J. M.; White, D. P.; Coville, N. J. *S. Afr. J. Chem.* **1997**, *50*, 59−66.
(22) Taverner, B. C. *J. Comput. Chem.* **1996**, *17*, 1612−1623.
(23) White, D.; Taverner, B. C.; Coville, N. J.; Wade, P. W. *J. Organomet. Chem.* **1995**, *495*, 41−51.
(24) White, D.; Tavener, B. C.; Leach, P. G. L.; Coville, N. J. *J. Organomet. Chem.* **1994**, *478*, 205−211.
(25) White, D.; Taverner, B. C.; Leach, P. G. L.; Coville, N. J. *J. Comput. Chem.* **1993**, *14*, 1042−1049.
(26) Brown, T. L.; Lee, K. J. *Coord. Chem. Rev.* **1993**, *128*, 89−116.
(27) Choi, M. G.; Brown, T. L. *Inorg. Chem.* **1993**, *32*, 5603−5610.
(28) Brown, T. L. *Inorg. Chem.* **1992**, *31*, 1286−1294.
(29) White, D. P.; Anthony, J. C.; Oyefeso, A. O. *J. Org. Chem.* **1999**, *64*, 7707−7716.
(30) Angermund, K.; Baumann, W.; Dinjus, E.; Fornika, R.; Görls, H.; Kessler, M.; Krüger, C.; Leitner, W.; Lutz, F. *Chem. Eur. J.* **1997**, *3*, 755−764.
(31) Reetz, M. T.; Haderlein, G.; Angermund, K. *J. Am. Chem. Soc.* **2000**, *122*, 996−997.
(32) Koide, Y.; Bott, S. G.; Barron, A. R. *Organometallics* **1996**, *15*, 2213−2226.
(33) Akai, I.; Sakakibara, K.; Hirota, M. *Chem. Lett.* **1992**, 1317−1320.
(34) Komatsuzaki, T.; Akai, I.; Sakakibara, K.; Hirota, M. *Tetrahedron* **1992**, *48*, 1539−1556.
(35) Hirota, M.; Sakakibara, K.; Komatsuzaki, T.; Akai, I. *Comput. Chem.* **1991**, *15*, 241−248.
(36) Komatsuzaki, T.; Sakakibara, K.; Hirota, M. *Chem. Lett.* **1990**, 1913−1916.
(37) Komatsuzaki, T.; Sakakibara, K.; Hirota, M. *Tetrahedron Lett.* **1989**, *30*, 3309−3312.

Table 1. Calculated Steric Values for Several Monodentate (Top) and Bidentate (Bottom) 3,4-Diazaphospholanes and Some Standard Phosphines[a]

phosphine	Ω[b]	%[c]	θ[d]	phosphine	Ω	%	θ	phosphine	Ω	%	θ
$P(OMe)_3$	2.67	21.3	110	**21**	4.42	35.2	146	**9**	5.31	42.3	162
PMe_3	2.74	21.8	111	**1**[e]	4.54	35.7	148	$P(mesityl)_3$	5.78	46.0	171
PPh_3	3.53	28.1	128	**15**	4.51	35.9	147	**14**	5.85	46.6	172
2	3.87	30.8	135	$P(o\text{-tolyl})_3$	4.76	37.9	152				
3	4.34	34.6	144	$P(t\text{-Bu})_3$	5.03	40.1	157				
DPPM	4.30	34.3	143	BINAP	5.17	41.2	160	**17**	6.75	53.7	188
Me-DuPhos	5.03	40.0	157	DCPB	5.76	45.8	170	D(*t*-Bu)PF	6.79	54.0	189
DPPB	5.17	41.1	160	**16**	6.47	51.5	183				

[a] Abbreviations: DPPM = bis(diphenylphosphino)methane; DPPB = bis(diphenylphosphino)butane; DCPB = bis(dicyclohexylphosphino)butane; D(*t*-Bu)PF = 1,1′-bis(di-*tert*-butylphosphino)ferrocene. [b] Solid angle. [c] Area percent. [d] Solid-G cone angle. [e] This phosphine crystallized as a mixture of two different isomers: one isomer with both NHs cis and the other isomer with the NHs trans. The numbers in the table represent an average of the values for both conformational isomers.

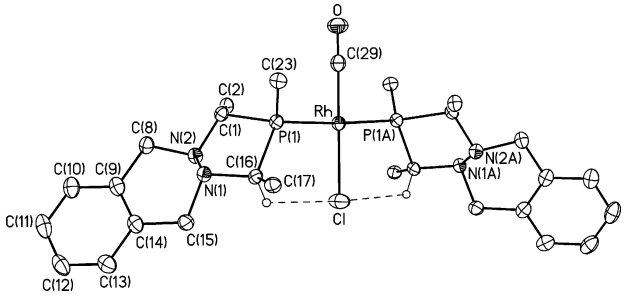

Figure 3. ORTEP drawing of compound **23**. Thermal ellipsoids are drawn at the 50% probability level. All hydrogen atoms are omitted, except for the hydrogens that interact with the chlorine. The dashed lines indicate the hydrogen-bonding interaction. Only the ipso carbon atoms of the Ph groups are shown.

Utilizing X-ray crystallographic data, we calculated the steric parameters for several 3,4-diazaphospholanes. For comparison, the steric parameters of some standard monodentate and bidentate phosphines also were calculated from crystallographic structures deposited in the Cambridge Structural Database (CSD). Table 1 presents normalized steric measurements of 3,4-diazaphospholanes and standard phosphines. Inspection of the data reveals some interesting features. Diazaphospholanes are bulky; the smallest diazaphospholane measured, *rac*-**2** (θ = 135°), is larger than PPh_3 (θ = 128°). In fact, most of the diazaphospholanes have sizes that are comparable to some of the largest standard phosphines. Protection of nitrogen atoms as carboxamides does not affect the steric size, although it increases the rigidity and chemical stability of the ligand backbone. For example, compounds *rac*-**1**, *rac*-**3**, and *rac*-**13**, which are identical except for the functionalization of the nitrogens, have similar cone angles.

To elucidate structural changes resulting from reduction of carboxamide-protected 3,4-diazaphospholanes, $[Rh(rac\text{-}\mathbf{21})_2(CO)Cl]$ (**23**) was synthesized (vide infra) and structurally characterized by crystallography. The crystallographic structure and selected distances and angles are presented in Figure 3 and Table 2, respectively. Steric parameters of the phosphine show little change after reduction of *rac*-**3** to *rac*-**21** (Table 1). Structures of *rac*-**21** and *rac*-**3** were analyzed with the program Platon.[38] Results are in Table 3. As expected, reducing the carbonyl carbon (sp^2) to a methylene (sp^3) causes a dramatic change in the puckering amplitude, Q,[39] of the six-membered diazacyclohexane ring: Q = 0.151 Å for *rac*-**3** versus Q = 0.593 Å for *rac*-**21**. Both *rac*-**3** and *rac*-**21** display approximately the same five-membered diazaphospholane ring-puckering amplitudes: Q = 0.445 Å (*rac*-**21**) and Q = 0.408(41) Å (*rac*-**3**). Significant changes are seen in the orientation of the phenyl rings in the 2- and 5-positions of the diazaphospholane ring, as determined by the angle (φ) of the substituents to the least-squares plane of the phospholane ring.[40,41] The diazaphospholane *rac*-**3** has one phenyl ring in the axial position (φ = 78(4)°), whereas the other phenyl group is bisectionally positioned (φ = 36(3)°). After reduction, the bisectionally oriented phenyl ring stays in place (φ = 37°), but the other moves to an equatorial orientation (φ = 28°). For comparison, we analyzed several structures from the CSD of 2,5-dimethyl-1-phenylphospholane (**24**).[42,43] The methyl substituents of **24** are also equatorial (φ = 22(4)°) and bisectional (φ = 44(10)°). It seems clear that the borane reduction has converted the original 3,4-diazaphospholane into a structure that more closely resembles DuPHOS and related phospholanes. The orientation of the groups at the 2- and 5-positions is presumably the major influence on enantioselection during metal-catalyzed reactions, and the reorientation of these substituents may have a dramatic effect on the enantioselectivities obtained in metal-catalyzed reactions. These predictions will be tested experimentally.

Diazaphospholane Electronic Effects. Reaction of $[Rh(CO)_2Cl]_2$ with 2 equiv of phosphine (PR_3) per rhodium in CH_2Cl_2 generates the square-planar complexes $[trans\text{-}Rh(PR_3)_2(CO)Cl]$. The IR carbonyl stretching frequencies of these complexes provides a measure of the electron-donating abilities of the phosphines. There are numerous examples of these types of complexes in the literature; therefore, comparisons with many standard phosphines can be made.[44−46] Unfortunately, the CO stretching frequencies of such Rh complexes are not purely sensitive to ligand electronics and can be sensitive to the size of the ligands. For example, the coordination framework of the complex $[trans\text{-}Rh(P(t\text{-}Bu)_3)_2(CO)Cl]$ is distorted from an idealized square plane, making the carbonyl stretch inconsistent with complexes of less bulky phosphines.[47,48]

(38) Spek, A. L. *J. Appl. Crystallogr.* **2003**, *36*, 7−13.
(39) Cremer, D.; Pople, J. A. *J. Am. Chem. Soc.* **1975**, *97*, 1354−1358.
(40) These angles are opposite those used in the literature, so that they would be easier to describe and understand. Angles of 0−30° are equatorial, 30−60° are bisectional, and 60−90° are axial.
(41) Luger, P.; Bülow, R. *J. Appl. Crystallogr.* **1983**, *16*, 431−432.
(42) Burk, M. J.; Feaster, J. E.; Harlow, R. L. *Tetrahedron: Asymmetry* **1991**, *2*, 569−592.
(43) Burk, M. J.; Feaster, J. E.; Harlow, R. L. *Organometallics* **1990**, *9*, 2653−2655.
(44) Smith, D. C., Jr.; Stevens, E. D.; Nolan, S. P. *Inorg. Chem.* **1999**, *38*, 5277−5281.
(45) Vastag, S.; Heil, B.; Markó, L. *J. Mol. Catal.* **1979**, *5*, 189−195.
(46) Marinetti, A.; Labrue, F.; Pons, B.; Jus, S.; Ricard, L.; Genêt, J.-P. *Eur. J. Inorg. Chem.* **2003**, 2583−2590.
(47) Harlow, R. L.; Westcott, S. A.; Thorn, D. L.; Baker, R. T. *Inorg. Chem.* **1992**, *31*, 323−326.
(48) Schumann, H.; Heisler, M.; Pickardt, J. *Chem. Ber.* **1977**, *110*, 1020−1026.

Table 2. Selected Bond Distances (Å) and Angles (deg) for Complexes 23, 25, 26, and 29

23		25		26		29	
Rh−P(1)	2.3142(4)	Rh−P	2.2576(9)	Rh−P	2.2467(9)	Rh(1)−P(1)	2.195(3)
Rh−Cl	2.3640(6)	Rh−Cl(1)	2.3497(8)	Rh−Cl	2.3345(10)	Rh(1)−P(2)	2.181(3)
Rh−C(29)	1.819(2)	Rh−C(30)	2.104(3)	Rh−C(1)	2.094(4)	Rh(1)−Cl(1)	2.403(3)
O−C(29)	1.132(3)	Rh−C(36)	2.106(3)	Rh−C(2)	2.093(4)	Rh(1)−Cl(1)#1	2.405(3)
		Rh−C(33)	2.194(3)	Rh−C(6)	2.206(4)		
		Rh−C(32)	2.201(3)	Rh−C(7)	2.203(4)		
		C(30)−C(36)	1.393(5)	C(1)−C(2)	1.392(6)		
		C(32)−C(33)	1.358(5)	C(6)−C(7)	1.358(6)		
P(1)−Rh−Cl	91.644(10)	P−Rh−Cl(1)	93.60(3)	P−Rh−Cl	94.88(4)	P(2)−Rh(1)−P(1)	94.26(11)
P(1)−Rh−C(29)	88.356(10)	P−Rh−C(30)	102.52(10)	P−Rh−C(1)	96.46(12)	P(1)−Rh(1)−Cl(1)#1	93.81(10)
C(29)−Rh−Cl	180.0	P−Rh−C(36)	94.65(10)	P−Rh−C(2)	98.38(11)	Cl(1)−Rh(1)−Cl(1)#1	81.22(10)
		C(30)−Rh−C(32)	66.25(14)	C(1)−Rh−C(6)	66.50(16)	P(2)−Rh(1)−Cl(1)	92.22(10)
		C(36)−Rh−C(33)	66.74(13)	C(2)−Rh−C(7)	66.75(15)		
		C(32)−Rh−Cl(1)	95.92(10)	C(6)−Rh−Cl	96.90(11)		
		C(33)−Rh−Cl(1)	96.92(9)	C(7)−Rh−Cl	95.43(10)		

Table 3. Structural Features of the Phospholane Rings of 21, 3, and 24

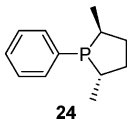

24

	Q[a]		*φ*[b]	
phosphine	phospholane[c]	diazacyclohexane[d]	2-substituent[e]	5-substituent[e]
3	0.409(41)	0.151(16)	78(4)	36(3)
21	0.445	0.593	37	28
24	0.447(12)		44(10)	22(4)

[a] *Q* = puckering amplitude in Å. Average deviations of the atoms in the ring from the least-squares plane are shown, with standard deviations of *Q* given in parentheses. [b] Angles (in deg) of the substituents in the 2- and 5-positions of the phospholane ring relative to the least-squares plane of the five atoms that make up the phospholanes. [c] Five-membered ring containing the phosphorus. [d] Six-membered ring formed between the hydrazine and the phenyl ring. [e] The 2-substituent was arbitrarily chosen to be the substituent with the largest *φ* value.

Table 4. IR Carbonyl Stretching Frequencies of the Complexes Rh(phosphine)$_2$(CO)Cl for 3,4-Diazaphospholanes (Top) and Standard Phosphines (Bottom)

phosphine	*ν*(CO) (cm^{-1})[a]	*δ*(^{31}P) (ppm)[b]	J_{P-Rh} (Hz)
22	1968	56.4	128
		55.6	127
11	1975	49.3	131
		49.1	132
12	1976	44.9	141
10	1980	58.3	139
21	1982	52.3	140
		54.7	138
5	1988	36.8	139
3	1990	46.6	135
		45.4	134
6	1994	40.1	125
		38.9	124
8	1997	48.8	144
7	2011	52.7	144
P(Cy)$_3$[44]	1942		
24[46]	1963		
PMe$_2$Ph[44]	1968		
PPh$_3$[44,45]	1978		
P(OPh)$_3$[45]	2016		

[a] All IR data was collected in CH_2Cl_2 in a CaF_2 solution cell. [b] All ^{31}P NMR data were collected unlocked in CH_2Cl_2.

The [*trans*-Rh(PR$_3$)$_2$(CO)Cl] complexes of several of the 3,4-diazaphospholanes were prepared and analyzed. Carbonyl stretching frequencies and ^{31}P NMR data are given in Table 4. The carbonyl stretching data clearly show that 3,4-diazaphospholanes are electron-poor, having electronic properties that fall somewhere between those of triarylphosphines and triaryl phosphites.

Some, but not all, of the [*trans*-Rh(3,4-diazaphospholane)$_2$(CO)Cl] complexes (e.g., with 3,4-diazaphospholanes **3**, **6**, **11**, **21**, and **22**) exhibit two ^{31}P NMR resonances. The use of racemic phosphines should give two diastereomeric rhodium complexes: one where both phosphines have the same absolute configuration (homochiral) and one where the phosphines have different absolute configurations (heterochiral). The presence of two diastereomers will yield two different ^{31}P chemical shifts. The factors that lead to the formation of only one diastereomer for phosphines *rac*-**5**, *rac*-**7**, *rac*-**8**, *rac*-**10**, and *meso*-**12** are unknown.

Attempted syntheses of the rhodium complex with the extremely bulky, but presumably electron rich, *meso*-**12** led to two products in low yield. The ^{31}P NMR spectrum of the reaction solution shows mostly unreacted *meso*-**12** (−5.8 ppm) together with two small doublets (38.5 and 44.9 ppm), and the IR spectrum of this mixture shows multiple carbonyl stretching frequencies. These observations are consistent with either the formation of both the mono- and bis-phosphine rhodium complexes,[49,50] or with cis and trans isomers of a mono-phosphine rodium complex. To distinguish between these possiblities, a solution of [Rh(CO)$_2$Cl]$_2$ was titrated with *meso*-**12** while recording the ^{31}P NMR and FTIR. The doublet at 44.9 ppm increases in intensity relative to the doublet at 38.5 ppm as the amount of phosphine is increased. The dependence of product ratios on the P:Rh ratio suggests a mixture of mono- and bis-phosphine rhodium complexes, the doublet at 44.9 ppm in the ^{31}P NMR corresponding to [*trans*-(*meso*-**12**)$_2$Rh(CO)Cl] and the doublet at 38.5 ppm corresponding to [(*meso*-**12**)Rh(CO)$_2$Cl]. The presence of a cis−trans isomer equilibrium mixture can be ruled out by the concentration dependence of the ratio of species as determined by ^{31}P NMR; a mixture of mono- and bis-phosphine adducts requires their ratio to be dependent on free phosphine concentration. The FTIR data for the CO stretching region can be interpreted as follows. The peaks at 2094 and 2016 cm^{-1}, which have approximately equal intensities, are assigned to the symmetric and antisymmetric vibrations, respectively,[51] of [(*meso*-**12**)Rh(CO)$_2$Cl]. The FTIR

(49) Prókai-Tátrai, K.; Torös, S.; Heil, B. *J. Organomet. Chem.* **1987**, *332*, 331−335.
(50) Braunstein, P.; Heaton, B. T.; Jacob, C.; Manzi, L.; Morise, X. *Dalton Trans.* **2003**, 1396−1401.
(51) Beckerle, J. D.; Casassa, M. P.; Cavanagh, R. R.; Heilweil, E. J.; Stephenson, J. C. *Chem. Phys.* **1992**, *160*, 487−497.

Scheme 3. General Synthesis of 25 and 26

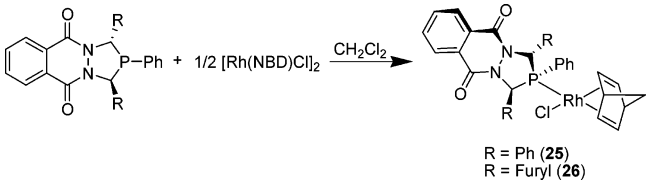

absorption at 1976 cm^{-1} is assigned to [*trans*-(*meso*-**12**)$_2$Rh(CO)Cl]. This assignment is based on both the expected frequency for a [(phosphine)$_2$Rh(CO)Cl] complex and the observation of increased intensity relative to the peaks at 2016 and 2094 cm^{-1} as the free phosphine concentration increases. The compounds [*trans*-(*meso*-**12**)$_2$Rh(CO)Cl] and [*trans*-(*rac*-**11**)$_2$Rh(CO)Cl] exhibit identical CO stretching frequencies, which suggests that substitution of the *tert*-butyl group with an isopropyl group and the change of stereochemistry from *rac* to *meso* have little effect on the electronic properties of these phosphines.

Substitution of the phenyl groups in the 2- and 5-positions of the diazaphospholane ring (**3** and **10**) with isopropyl groups (**5** and **11**) has only a small effect on the overall electronics of the system (2−5 cm^{-1}). Replacing the phenyl ring directly attached to the phosphine (**3** and **5**) with a cyclohexyl group (**10** and **11**) induces a more substantial change in electronics (10−13 cm^{-1}). Interestingly, the most electron-rich, unreduced 3,4-diazaphospholane (**10**) is substantially more electron-deficient than **24**,[46] which is the monodentate analogue of DuPHOS.

Comparison of the reduced diazaphospholanes *rac*-**22** and *rac*-**21** with their unreduced analogues *rac*-**3** and *rac*-**10** reveals an approximately 10 cm^{-1} decrease in the carbonyl stretching frequency after reduction. Considering that the total range of known stretching frequencies for these types of complexes is approximately 80 cm^{-1}, a change of 10 cm^{-1} corresponds to a substantial increase in the electron-donating ability of the phosphine. Overall, in combination with the borane-reduction modification, the 3,4-diazaphospholanes have carbonyl stretching frequencies that cover about 60% of the total range of frequencies spanned by the combination of phosphines and phosphites.

Synthesis of Rhodium Complexes. The air-stable, orange rhodium(I) complexes **25** and **26** were prepared quantitatively by reacting the corresponding 3,4-diazaphospholane with 0.5 equiv of [Rh(NBD)Cl]$_2$ (NBD = bicyclo[2.2.1]hepta-2,5-diene) in CH_2Cl_2 (Scheme 3). X-ray-quality crystals of **25** and **26** were grown by the slow diffusion of hexanes into a CH_2Cl_2 solution of the metal complex; the crystallographic structures are presented in Figures 4 and 5, respectively, and selected structural metrics are presented in Table 2. Both compounds show similar spectroscopic and structural characteristics; therefore, only the analysis of compound **25** will be presented. The ^{31}P NMR resonance of **25** was observed as a doublet at 45 ppm (J_{P-Rh} = 189 Hz). The olefinic CH resonances of the complexed norbornadiene are inequivalent in the ^1H NMR spectrum, and as expected, CH resonances cis to the phosphine appear at 3.06 and 3.34 ppm, while the CH resonances trans to the phosphine are shifted downfield to 5.10 and 5.22 ppm. The trans influence can also be seen in the Rh−C_{olefin} bond distances: 2.194(3) and 2.201(3) Å for the trans carbons and 2.104(3) and 2.106(3) Å for the cis carbons. An interesting structural feature is the short separation of the chloride ligand and a methine hydrogen of the diazaphospholane ring, H−C(P)(N): the Cl···H distance, 2.72 Å, is significantly shorter than the sum of the van der Waals radii (2.95 Å), which suggests a C−H···Cl hydrogen-bonding interaction.[52] The C−H···Cl angle is 128°, which is much smaller than the optimum H-bond angles (165−180°), but examples of H bonding with smaller angles (120−128°) are not unusual.[52] We speculate that such unusual intramolecular C−H···Cl interactions are due to the polarization of the C−H bond by the geminal phosphorus and nitrogen. These interactions are not limited to complex **25**; many 3,4-diazaphospholane complexes display similar interactions (Table 5).

Complex **25** does not react with excess *rac*-**3**; however, if AgOTf (OTf = trifuloromethanesulfonate) is added to a mixture

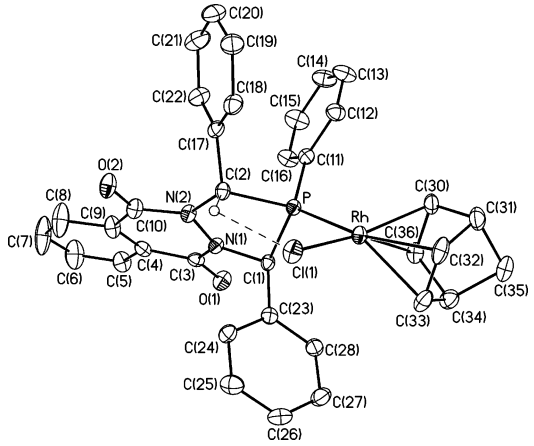

Figure 4. ORTEP drawing of compound **25**. All hydrogen atoms are omitted, except the hydrogen that interacts with the chlorine. The dashed line indicates the hydrogen-bonding interaction. Thermal ellipsoids are drawn at the 30% probability level.

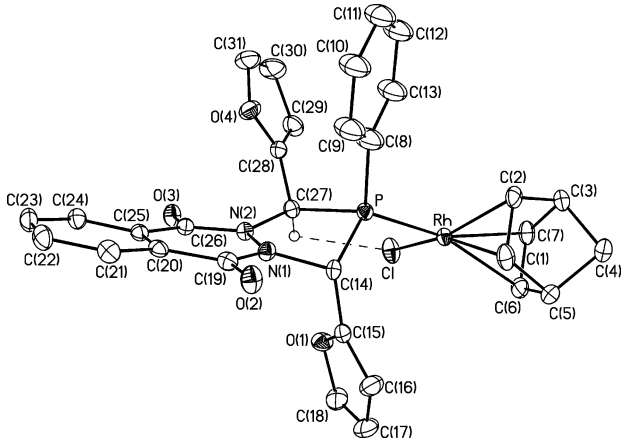

Figure 5. ORTEP drawing of compound **26**. All hydrogen atoms are omitted, except the hydrogen that interacts with chlorine. The dashed line indicates the hydrogen-bonding interaction. Thermal ellipsoids are drawn at the 30% probability level.

Table 5. Intramolecular Cl···H Interactions in 23, 25, 26, 28, and 33

	A···H[a]	A···D[b]	A···H-D[c]
23	2.73	3.411(2)	126
25	2.72	3.419(3)	128
26	2.77	3.408(4)	122
28	2.68	3.40(1)	128
	2.65	3.39(2)	130
33	2.71	3.452(3)	131
	1.82[d]	2.653(3)[d]	172[d]

[a] Hydrogen−acceptor distance in Å. [b] Acceptor−donor distance in Å. [c] Donor−hydrogen−acceptor angle in deg. [d] Intermolecular hydrogen-bonding interaction between the phenolic OH and the amide carbonyl.

(52) Steiner, T. *Angew. Chem., Int. Ed.* **2002**, *41*, 48−76.

Scheme 4

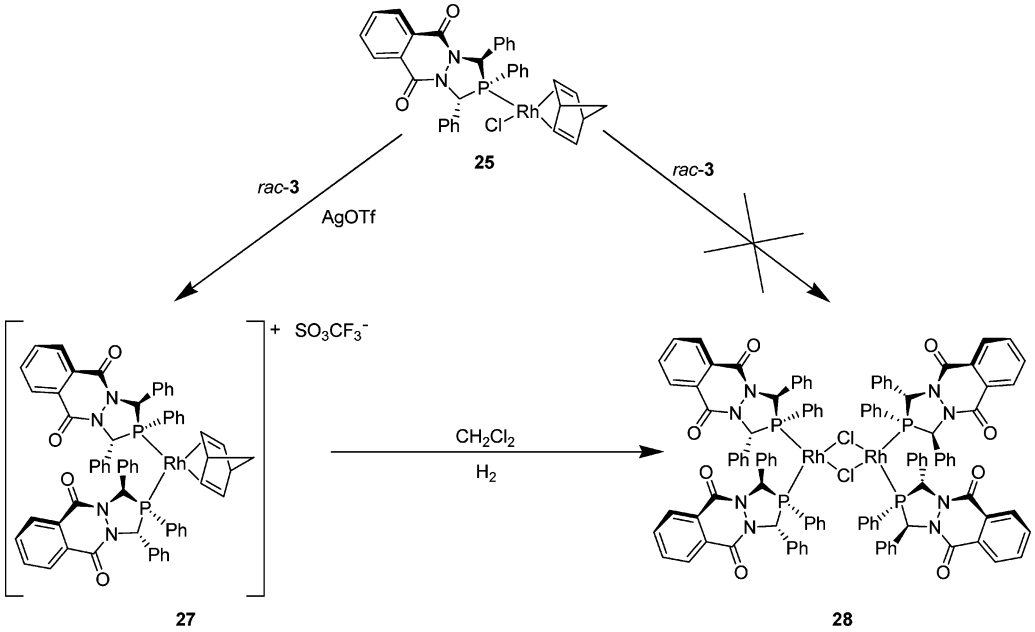

Scheme 5

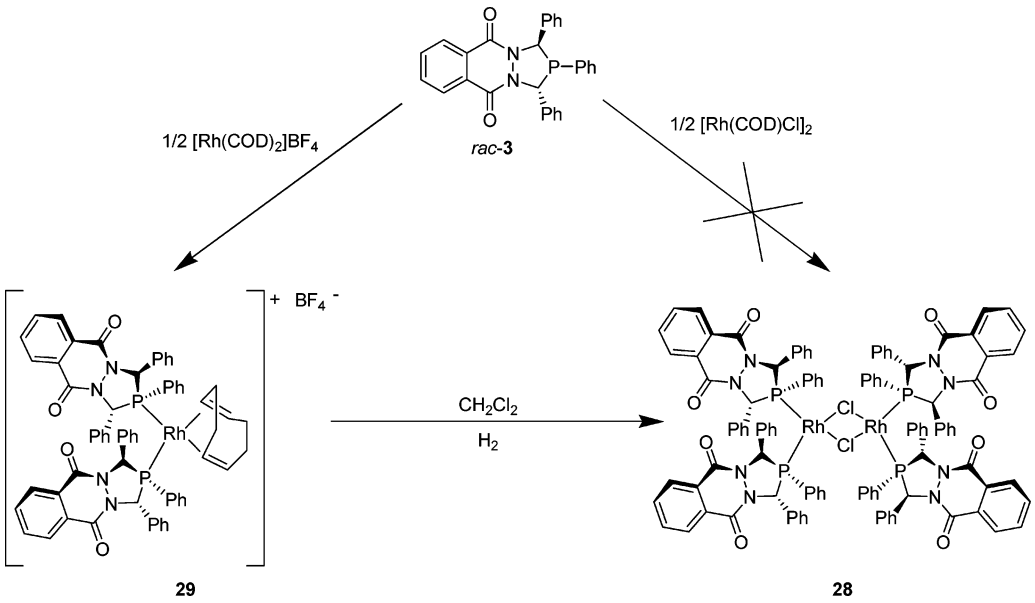

of **25** and *rac*-**3**, a new rhodium(I) complex is observed by ^{31}P NMR as a doublet (J_{P-Rh} = 163 Hz) at 49 ppm. On the basis of the Rh−P coupling constant and the ^{1}H NMR spectrum, this compound was assigned as the cationic, homochiral rhodium-(I) complex **27**. Interestingly, recrystallization of this complex from CH_2Cl_2 with hexanes gave X-ray-quality crystals that were not **27** but the chloride-bridged dimer **28** (Scheme 4). The ^{1}H and ^{31}P NMR data corroborated this change (vide infra). Similarly, the reaction of 2 equiv of *rac*-**3** and $[Rh(COD)_2]BF_4$ (COD = 1,5-cyclooctadiene) in CH_2Cl_2 gave a product with initial ^{1}H and ^{31}P NMR data indicating the formation of the cationic, homochiral complex **29**; however, this complex also slowly decomposed to the chloride dimer **28**. For complexes **29** and **27**, treatment with hydrogen gas accelerated the chloride abstraction (Scheme 5). Activation of chlorinated solvents by Rh(I) complexes is not unprecedented,[53−60] but most examples yield the product of oxidative addition.[53−56,58−60] Generally, oxidative addition of CH_2X_2 (X = Cl, Br, I) to Rh(I) is enhanced by electron-donating ligands, but as our data have established (vide supra), the 3,4-diazaphospholanes are electron deficient, which argues against an oxidative addition pathway. Less abundant are examples of methylene chloride activations that

(53) Friedrich, H. B.; Moss, J. R. *Adv. Organomet. Chem.* **1991**, *33*, 235−290.

(54) Dorta, R.; Shimon, L. J. W.; Rozenberg, H.; Milstein, D. *Eur. J. Inorg. Chem.* **2002**, 1827−1834.

(55) Chan, K. T. K.; Spencer, L. P.; Masuda, J. D.; McCahill, J. S. J.; Wei, P.; Stephan, D. W. *Organometallics* **2004**, *23*, 381−390.

(56) Brunet, J. J.; Couillens, X.; Daran, J. C.; Diallo, O.; Lepetit, C.; Neibecker, D. *Eur. J. Inorg. Chem.* **1998**, 349−353.

(57) Hunt, C.; Fronczek, F. R.; Billodeaux, D. R.; Stanley, G. G. *Inorg. Chem.* **2001**, *40*, 5192−5198.

(58) Haarman, H. F.; Ernsting, J. M.; Kranenburg, M.; Kooijman, H.; Veldman, N.; Spek, A. L.; van Leeuwen, P. W. N. M.; Vrieze, K. *Organometallics* **1997**, *16*, 887−900.

(59) Bradd, K. J.; Heaton, B. T.; Jacob, C.; Sampanthar, J. T.; Steiner, A. *J. Chem. Soc., Dalton Trans.* **1999**, 1109−1112.

(60) Tejel, C.; Ciriano, M. A.; Oro, L. A.; Tiripicchio, A.; Ugozzoli, F. *Organometallics* **2001**, *20*, 1676−1682.

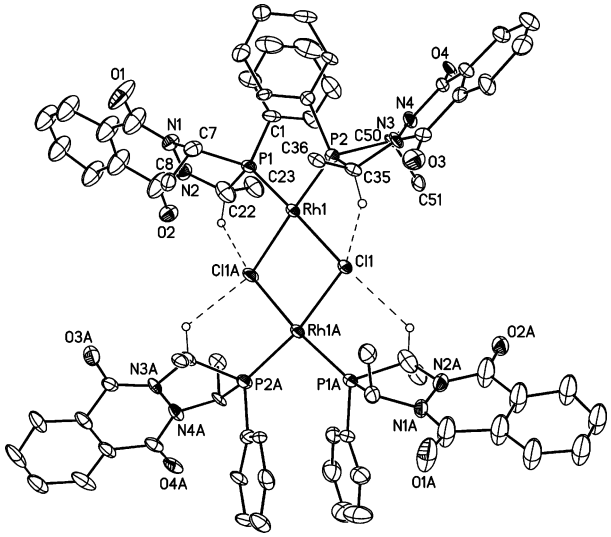

Figure 6. ORTEP drawing of compound **28**. All hydrogen atoms are omitted, except the hydrogens that interact with the chlorines. The dashed lines indicate hydrogen-bonding interactions. Only the ipso carbons are shown for the phenyl rings in the 3- and 5-positions of the diazaphospholane. Thermal ellipsoids are drawn at the 30% probability level.

only add chlorides to the rhodium,[57−60] and to the best of our knowledge, there are no examples of chloride abstractions without a change in formal oxidation state. The few examples of chloride abstractions in the literature postulate a possible radical mechanism.[57,58] Vrieze and co-workers[58] documented a reaction where a $[L_3RhCl]$ (L = tridentate amine) complex oxidatively added methylene chloride, the product of which was indefinitely stable under rigorous air-free conditions. Upon exposure to O_2 and water, however, it decomposes to $[L_3RhCl_3]$. We find that **27** and **29** are stable on the Schlenk line for several days, but when the flasks were set aside for recrystallization (which presumably exposes the solutions to small amounts of O_2), they abstract chloride from CH_2Cl_2 to give **28**. Such behavior suggests a radical mechanism for the halide abstraction.

Detailed NMR and crystallographic structural analyses performed on **28** reveal interesting structural features. There are no rhodium-bound alkenes in the ^{1}H NMR spectrum; the ^{31}P NMR resonance is a doublet (J_{P-Rh} = 215 Hz) at 58.2 ppm, consistent with a single diasteromer. The crystallographic structure and selected structural information are presented in Figure 6 and Table 2, respectively. The crystallographic structure is that of a homochiral complex, which suggests that the single diasteromer observed in solution by ^{31}P NMR is the homochiral diastereomer. Again, both chlorides hydrogen bond with neighboring H−C(P)(N) units from the diazaphospholanes: the Cl···H distances are 2.65 and 2.68 Å (Table 5). There also appears to be a series of three intramolecular π stacking interactions, which form a helix around the outside of the complex (Figure 7).[61−65] The central interaction is a $\pi-\pi$ stacking interaction, where the phenyl ring centroids (C_n1-C_n29[66]) are separated by 3.69 Å. The outer interactions are more accurately described

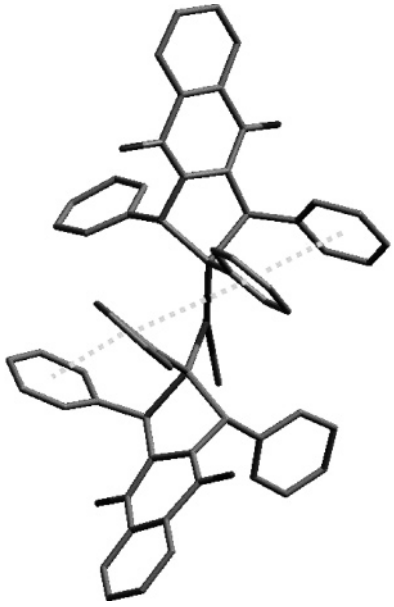

Figure 7. Phenyl ring interactions in **29**. Half of the complex and hydrogen atoms were removed for clarity. The dotted line represents the phenyl ring interactions.

Table 6. Phenyl Ring Interactions in 29

Ph(A)−Ph(B)[a]	C_n-C_n[b]	H−C_n[c]	∠$C_n-C_n-P_n$[d]	∠P−P[e]
Ph(1−6)−Ph(23−29)	3.97	3.15	38.2	25.4
Ph(1−6)−Ph(29−35)	3.69		26.9	10.14
Ph(29−35)−Ph(36−42)	4.33	2.80	53.3	31.5

[a] Descriptor for the phenyl rings based on their carbon numbering in the crystal structure. [b] Centroid−centroid distance in Å. [c] The closest hydrogen−centroid distance between the two rings. [d] The angle made by the vector between the two centroids and the normal to a least-squares plane of one of the phenyl rings (deg). [e] The angle between the least-squares planes made by the phenyl rings.

as C−H···π interactions. The H···C_n distances are H30···C_n36 = 2.80 Å and H6···C_n23 = 3.15 Å. Several other useful metrics for the π stacking interactions are presented in Table 6.

Unlike *rac*-**3** and *rac*-**6**, the 3,4-diazaphospholane *rac*-**15** has two functional groups that may potentially interact with bound substrates: the phenolic OH and the diazaphospholane NH. A mixture of *rac*-**15** with 0.5 equiv of $[Rh(COD)Cl]_2$ produced the previously described[67] complex **30** in quantitative yield (eq 2). X-ray-quality crystals of **30** were obtained by recrystalliza-

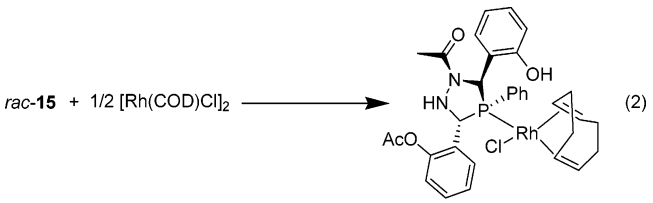

30

tion from CH_2Cl_2 with hexanes (Figure 8). Selected structural information is given in Table 7. The ^{31}P NMR resonance for **30** is a doublet (J_{P-Rh} = 154 Hz) at 67 ppm. Unlike the previous structures, however, **30** shows an intramolecular Cl···H−N interaction; the H···Cl distance is 2.341(13) Å, and the Cl···H−N angle is 152(2)°. There is also an intermolecular hydrogen bond between the phenol OH and the carbonyl of the lone amide

(61) Janiak, C. *Dalton Trans.* **2000**, 3885−3896.
(62) Hunter, C. A.; Sanders, J. K. M. *J. Am. Chem. Soc.* **1990**, *112*, 5525−5534.
(63) Janiak, C.; Temizdemir, S.; Dechert, S.; Deck, W.; Girgsdies, F.; Heinze, J.; Kolm, M. J.; Scharmann, T. G.; Zipffel, O. M. *Eur. J. Inorg. Chem.* **2000**, 1229−1241.
(64) Magistrato, A.; Pregosin, P. S.; Albinati, A.; Rothlisberger, U. *Organometallics* **2001**, *20*, 4178−4184.
(65) Meyer, E. A.; Castellano, R. K.; Diederich, F. *Angew. Chem., Int. Ed.* **2003**, *42*, 1210−1250.

(66) C_n# and P_n# are the centroid and normal of the phenyl ring, respectively, where # is the crystal structure label of the ipso carbon.

(67) Clark, R. W.; Guzei, I. A.; Jin, W. C.; Landis, C. R. *Acta Crystallogr., Sect. C: Cryst. Struct. Commun.* **2003**, *C59*, m144-m145.

Table 7. Selected Bond Distances (Å) and Angles (deg) for Complexes 30, 32, 33, and 35

30		**32**		**33**		**35**	
Rh−P	2.2943(6)	Rh(1)−P(1)	2.1458(13)	Pd−P	2.2939(6)	Pd−P(1)	2.2931(6)
Rh−Cl(1)	2.3856(7)	Rh(1)−P(2)	2.1494(13)	Pd−Cl	2.3704(7)	Pd−P(2)	2.1716(6)
Rh−C(5)	2.111(2)	Rh(2)−P(3)	2.1489(13)	Pd−C(1)	2.196(3)	Pd−Cl	2.3729(6)
Rh−C(6)	2.130(2)	Rh(2)−P(4)	2.1402(14)	Pd−C(3)	2.105(3)	Pd−C(45)	2.094(2)
Rh−C(1)	2.197(2)	Rh(1)−Cl(1)	2.3885(13)	Pd−C(2)	2.156(4)		
Rh−C(2)	2.235(2)	Rh(1)−Cl(2)	2.3887(13)	Pd−C(2′)	2.096(12)		
C(5)−C(6)	1.392(3)	Rh(2)−Cl(1)	2.3793(13)				
C(1)−C(2)	1.362(4)	Rh(2)−Cl(2)	2.3955(13)				
P−Rh−Cl(1)	92.97(2)	P(1)−Rh(1)−P(2)	85.28(5)	P−Pd−Cl	97.13(2)	P(1)−Pd−P(2)	86.51(2)
C(6)−Rh−P	91.45(7)	P(1)−Rh(1)−Cl(1)	92.83(5)	P−Pd−C(3)	97.85(10)	P(1)−Pd−Cl	96.09(2)
C(5)−Rh−P	94.10(7)	Cl(1)−Rh(1)−Cl(2)	85.50(4)	C1−Pd−C(1)	97.49(9)	Cl−Pd−C(45)	92.24(7)
C(6)−Rh−C(1)	81.77(9)	P(2)−Rh(1)−Cl(2)	96.52(5)	C(3)−Pd−C(1)	67.55(13)	C(45)−Pd−P(2)	85.77(7)
C(5)−Rh−C(2)	80.65(10)	P(3)−Rh(2)−P(4)	85.41(5)				
C(1)−Rh−Cl(1)	89.06(7)	P(3)−Rh(2)−Cl(1)	96.16(5)				
C(2)−Rh−Cl(1)	88.63(7)	Cl(1)−Rh(2)−Cl(2)	85.55(4)				
		P(4)−Rh(2)−Cl(2)	92.94(5)				

Scheme 6

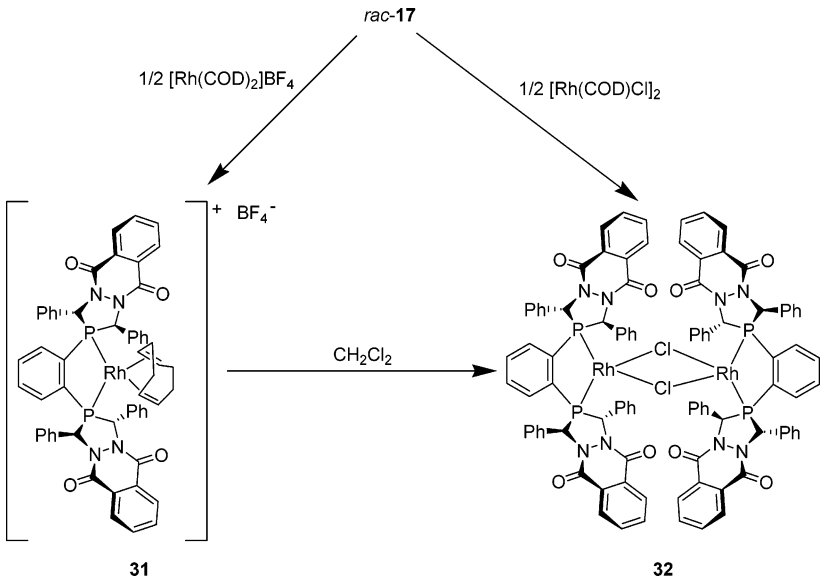

moiety, where the O−H···O═C distance is 1.82 Å and the O−H···O angle is 173°.

The stoichiometric reaction of the bis(3,4-diazaphospholane) *rac*-**17** with $[Rh(COD)_2]BF_4$ afforded [Rh(*rac*-**17**)(COD)]BF_4 (**31**) in quantitative yield. Compound **31** exhibits a ^{31}P resonance at 64 ppm (doublet, J_{P-Rh} = 165 Hz). Attempts to crystallize **31** in halogen-free solvents, such as THF and methanol, yielded only a glassy solid. As with complexes **27** and **29**, complex **31** decomposes in chlorinated solvents to afford the Cl-bridged, homochiral rhodium complex **32**, a process that takes almost 2 days to complete. Alternatively, we prepared compound **32** from the reaction of *rac*-**17** and $^1/_2[Rh(COD)Cl]_2$ (Scheme 6). The rhodium complex **32** was recrystallized from CH_2Cl_2/hexanes as yellow crystals. The X-ray structure (Figure 9, Table 7) shows no close contacts between Rh−Cl and H−C(P)(N). Restricted rotation around the Rh−P bond may prevent the H−C(P)(N) bond from interaction with the chlorides.

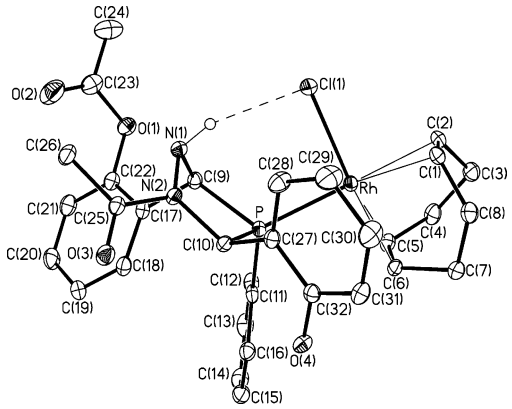

Figure 8. ORTEP drawing of compound **30**. All hydrogen atoms, except the N−H, are omitted. Thermal ellipsoids are drawn at the 30% probability level.

Synthesis of Palladium Complexes. The allyl complex [Pd(allyl)(*rac*-**15**)Cl] (**33**) was isolated quantitatively after reacting 0.5 equiv of $[Pd(allyl)Cl]_2$ with *rac*-**15** (eq 3). The ^{31}P

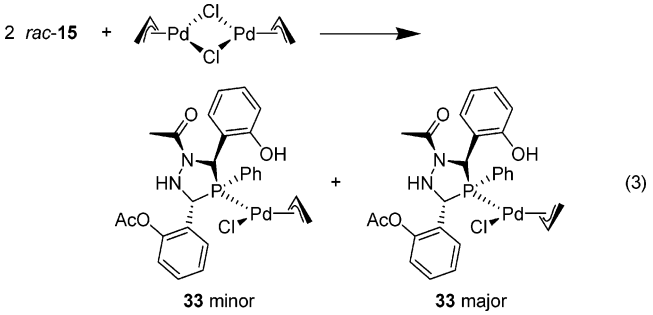

(3)

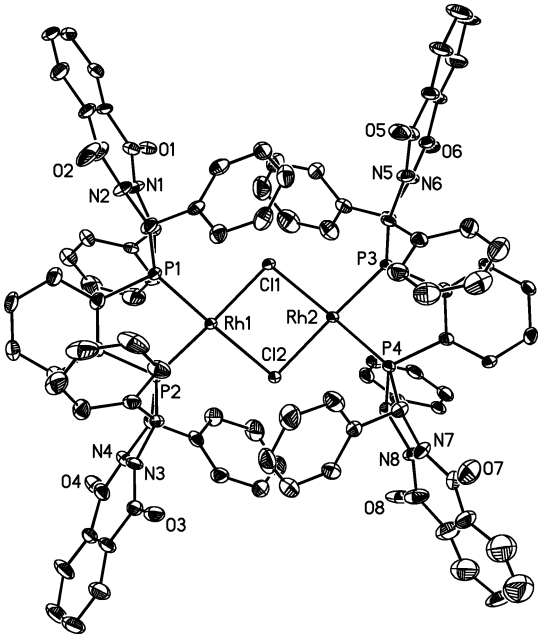

Figure 9. ORTEP drawing of compound **32**. All hydrogen atoms are omitted. Thermal ellipsoids are drawn at the 30% probability level.

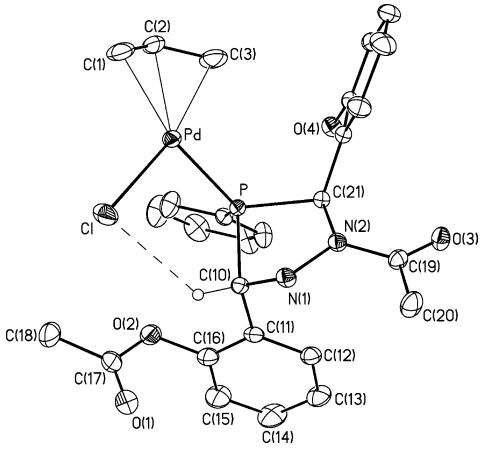

Figure 10. ORTEP drawing of compound **33** (major). All hydrogen atoms are omitted, except the hydrogen atoms that interact with the chlorine. The dashed line represents the hydrogen-bonding interaction. Thermal ellipsoids are drawn at the 30% probability level.

NMRspectrum has two broad singlets at 72.1 and 70.6 ppm, in a 1.4:1 ratio, consistent with two diastereomers that differ in the orientation of the allyl group with respect to the 3,4-diazaphospholane and the Pd coordination plane. Recrystallization from CH_2Cl_2/hexanes gave crystals suitable for X-ray structural characterization. The diastereomers **33** (major) and **33** (minor) cocrystallized in a 3:1 ratio. Figure 10 shows the X-ray structure of the major diastereomer, and Table 7 presents selected bond distances and angles. Unlike rhodium complex **30**, the chloride does not interact with the diazaphospholane N−H. Instead, the chloride hydrogen-bonds with H−C(P)(N): the Cl···H distance is 2.71 Å, and the C−H···Cl angle is 131° (Table 5). The Pd−$(CH_2)_{allyl}$ distance trans to the phosphorus (2.196(3) Å) is longer than the corresponding distance cis to the phosphorus (2.105(3) Å). The $(CH)_{allyl}$ group in the major diastereomer is positioned opposite the diazaphospholane ring relative to the square plane of the palladium, with a Pd−$(CH)_{allyl}$ bond distance of 2.156(4) Å. The $(CH)_{allyl}$ group in the minor diastereomer is on the same side as the diazaphospholane ring

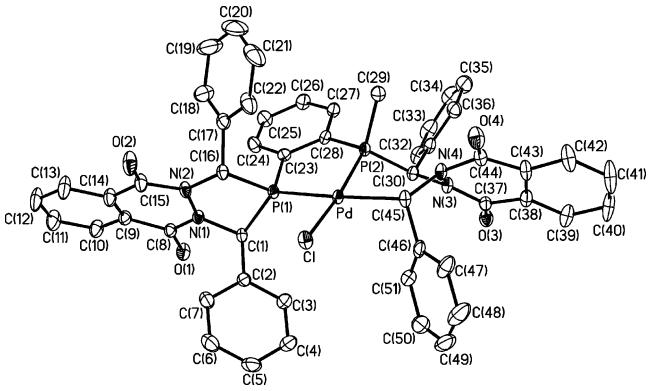

Figure 11. ORTEP drawing of compound **35**. All hydrogen atoms are omitted. Thermal ellipsoids are drawn at the 30% probability level.

Scheme 7

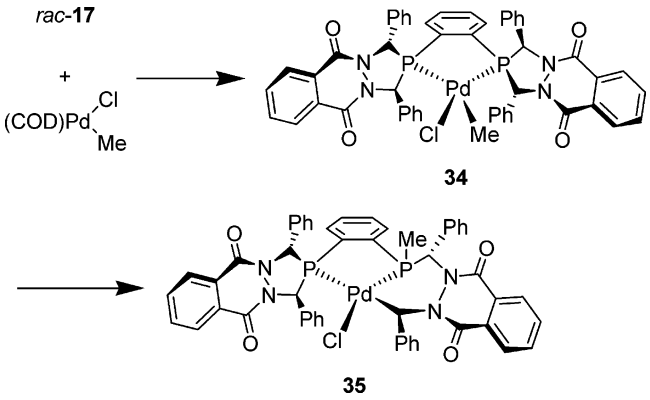

relative to the Pd coordination plane and has a correspondingly shorter Pd−$(CH)_{allyl}$ bond distance (2.096(12) Å).

The bis(3,4-diazaphospholane) *rac*-**17** displaces COD from [(COD)Pd(Me)Cl] to yield the yellow complex [(*rac*-**17**)Pd(Me)Cl] (**34**; Scheme 7). The ^{31}P NMR spectrum of this complex has two phosphorus resonances (64.7 and 42.8 ppm), indicative of asymmetric square-planar coordination around the palladium. Surprisingly, recrystallization from CH_2Cl_2/hexanes followed by crystallographic characterization yielded structure **35**, which is the product of a methyl migration to the phosphorus along with a ring opening of the diazaphospholane ring. Figure 11 illustrates the X-ray crystal structure of **35**, and Table 7 gives selected bond distances and angles. Two notable features of compound **35** are retention of stereochemistry at the methine carbons during migration and the stereoselective transfer of the methyl group to phosphorus. Monitoring the decomposition of **34** to **35** by NMR shows that this reaction is quite slow and is only complete after approximately 9 days.

Although C−P bond cleavage by transition metals has precedent in the literature,[68−71] phosphorus-heterocycle ring opening is rare.[69−71] To the best of our knowledge, there are no examples of phospholane ring opening in the literature. Glueck and co-workers, however, reported a metal-promoted opening of a chiral 2,4-diethylphosphetane ring to yield a metallacycle.[69] Two new stereogenic centers are formed: one at phosphorus and one at the metalated carbon. Of the four

(68) Garrou, P. E. *Chem. Rev.* **1985**, *85*, 171−185.
(69) Brunker, T. J.; Moncarz, J. R.; Glueck, D. S.; Zakharov, L. N.; Golen, J. A.; Rheingold, A. L. *Organometallics* **2004**, *23*, 2228−2230.
(70) Liedtke, J.; Rüegger, H.; Loss, S.; Grützmacher, H. *Angew. Chem., Int. Ed.* **2000**, *39*, 2478−2481.
(71) Mizuta, T.; Nakazono, T.; Miyoshi, K. *Angew. Chem., Int. Ed.* **2002**, *41*, 3897−3898.

Scheme 8. Possible Mechanisms for the Ring-Opening/Methyl Transfer Reaction

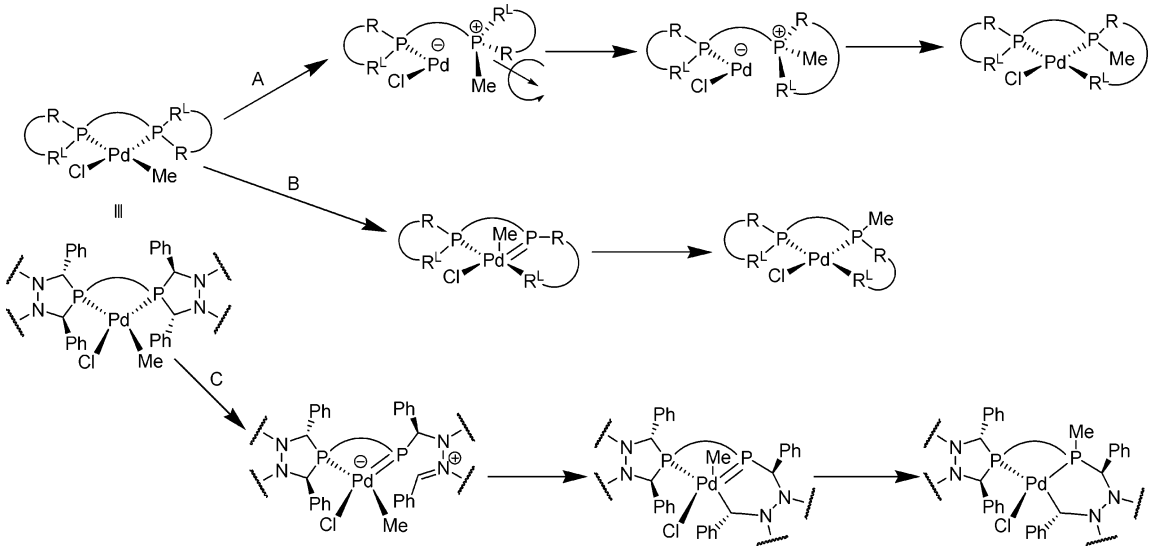

possible diastereomers, three are observed in a 6.3:2.7:1 ratio. This result is in contrast with the data observed for complex **35**, for which only one diastereomer is observed. There are two important points that can be drawn from the structure of **35**. First, the crystallographic structure confirms that none of the phospholane methines epimerized. Also, the new stereocenter generated at phosphorus has the same configuration as all of the methine carbons.

To help understand this ring-opening transformation, it is useful to employ a cartoon diagram of the reaction (eq 4). The

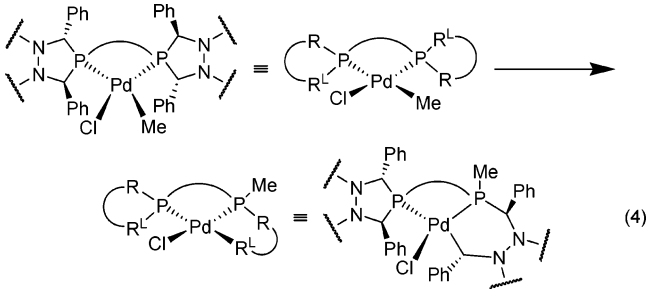

(4)

two diastereotopic P−C bonds of the diazaphospholane ring are labeled R and R^L, where R^L has the phenyl ring oriented toward the metal. We envision three possible mechanisms for this transformation, which are outlined in Scheme 8. Path A depicts a Pd(II)−Pd(0)−Pd(II) transformation in which an initial reductive elimination transfers the methyl group to the phosphorus, creating a zwitterion. Subsequent oxidative addition of either the P−R^L or P−R bond yields **35**. Another possible mechanism involves an initial oxidative addition of R^L, creating a five-coordinate Pd(IV) complex (Scheme 8, path B). Subsequent methyl insertion step must be stereoselective, because the methyl group should not pass through the newly formed R^L−Pd ring. A third mechanism is shown in path C. The coordinated 3,4-diazaphospholane undergoes an α elimination to give a iminium phosphide zwitterion. Palladium can then act as a nucleophile, attacking the iminium group and forming the six-membered ring. Unfortunately, our data do not allow distinction among these mechanisms.

Conclusions

In summary, we have found that the 3,4-diazaphospholanes are bulky and electron-deficient phosphine ligands. The cone angles of these ligands range from 135 to 188°, values that rival those of many of the largest standard phosphines. Perhaps it is the large steric sizes of these ligands that leads to some distinctive coordination chemistry of these phosphines with both rhodium(I) and palladium(II): the cationic rhodium(I) complexes **27**, **29**, and **31** abstract chloride from the solvent to form chloride-bridged dimers **28** and **32**, while the palladium(II) complex **34** rearranges by a combination of methyl transfer and ring opening to afford **35**. The electronic properties of the 3,4-diazaphospholanes, as determined by the infrared carbonyl stretching frequencies of [*trans*-Rh(3,4-diazaphospholane)$_2$(CO)Cl] complexes, span a broad range, with values between dialkylarylphosphines and dialkyl aryl phosphites (1975−2011 cm^{-1}). The electron-deficient nature of the 3,4-diazaphospholanes may partially explain the exceptional, phosphite-like activity these phosphines show in Rh-catalyzed hydroformylation.[13] In comparison with phosphites, 3,4-diazaphospholanes are less susceptible to hydrolysis under the hydroformylation reaction conditions. Reduction of the acyl protective group increases the electron-donating ability by approximately 10 cm^{-1} and reorients the diazaphospholane ring substituents. With respect to catalytic application these effects may be significant. In theory, reduction of the most electron-deficient 3,4-diazaphospholane, **11**, should provide access to electronic and steric properties similar to those of the DuPHOS family of ligands. It is expected that these changes will enable effective manipulation of both the reactivity and enantioselectivity obtained with 3,4-diazaphospholane-modified transition-metal catalysts.

Experimental Section

General Considerations. All organometallic complexes and phosphines were prepared under air- and moisture-free conditions using standard Schlenk-line techniques. The workup and flash chromatography were performed open to air. A circulating nitrogen-filled glovebox operating at <0.2 ppm of oxygen was used for long-term storage of these compounds. Phthaloyl and succinyl dichlorides were placed under vacuum (0.5 Torr) for 30 min to remove volatile impurities before storing them under N_2. Ether, THF, and hexanes were distilled from Na/benzophenone; CH_2Cl_2 was distilled over P_2O_5. $CDCl_3$ was purchased from Aldrich, distilled over calcium hydride, and vacuum-transferred into an airtight solvent bulb prior to transfer into the inert-atmosphere glovebag. All organometallic compounds and primary phosphines were purchased from Strem.

All other reagents were purchased from Aldrich and used without further purification.

Routine NMR characterization experiments—^{1}H, ^{13}C, and ^{31}P—were carried out on a Bruker AC-300, Varian Mercury-300, or a Varian Inova-500 instrument. ^{1}H NMR data are reported as follows: chemical shift (multiplicity (b = broad, s = singlet, d = doublet, t = triplet, q = quartet, p = pentet, s = sextet, sp = septet, o = octet, and m = multiplet), and integration). Chemical shifts for ^{1}H NMR spectra are reported in ppm downfield from internal tetramethylsilane (TMS, δ scale) using residual protons in the deuterated solvents (C_6D_6, 7.15 ppm; $CDCl_3$, 7.25 ppm; CD_2Cl_2, 5.31 ppm) as references. ^{13}C and ^{31}P NMR spectra were determined with ^{1}H decoupling and the chemical shifts are reported in ppm vs Me_4Si ($CDCl_3$ at 77 ppm and C_6D_6 at 128 ppm) and 85% H_3PO_4 standard (external, 0 ppm), respectively. IR spectra were recorded as CH_2Cl_2 solutions in a CaF_2 solution cell on a Mattson Polaris FTIR spectrometer. Elemental analyses were provided by Desert Analysis (Phoenix, AZ). Some compounds contain cocrystallized solvents by ^{1}H NMR, even after drying under vacuum overnight. These extra solvent molecules skewed the elemental analyses; however, on the basis of the ^{1}H NMR, we were able to determine the amount of residual solvent and take that into account with the elemental analysis data.

Compounds **1**−**4**, **6**, **7**, **13**−**15**, and **20**,[12] **9**,[14] **30**,[67] [Rh(COD)Cl]$_2$,[72−74] [Rh(NBD)Cl]$_2$,[75,76] [Rh(COD)$_2$]BF$_4$,[75,77,78] (COD)Pd(Me)Cl,[79,80] and azines[17] (except isopropyl) were all prepared by literature procedures.

Isopropyl Azine. Isobutyraldehyde (55 mmol, 5 mL) and hydrazine hydrate (27 mmol, 1.3 mL) were combined in benzene (30 mL), and the mixture was heated to reflux with a Dean−Stark trap. The reaction was monitored by collection of water in the Dean−Stark trap. Once complete, the benzene was removed under vacuum and the product was isolated by vacuum distillation (77−80 °C at 24 Torr). Yield: 77% (2.92 g, 20.8 mmol) of a clear, yellow oil. ^{1}H NMR (300 MHz, $CDCl_3$): δ 1.13 (d, J = 7 Hz, CHC*H*$_3$, 12H), 2.57 (pd, J = 7 Hz, 5 Hz, C*H*CH$_3$, 2H), 7.72 (d, J = 5 Hz, N=C*H*, 2H).

General Synthesis of Alkyldiazaphospholanes (*rac*-5, *rac*-11, and *meso*-11). Isopropyl azine (3.6 mmol), primary phosphine (3.5 mmol), and HCl (2 M in Et_2O, 3.6 mmol) were added to dry THF (25 mL), respectively. This mixture was stirred for 3 h before being cannula-transferred into a new flask containing an excess of finely ground K_2CO_3 (∼2 g). After it was stirred for 0.5 h, the reaction mixture was filtered into a new flask and phthaloyl dichloride (3.9 mmol) was added. After the solution was stirred for 12 h, the reaction mixture was cannula-transferred into a flask containing an excess of finely ground $Na_2CO_3 \cdot H_2O$ (∼2 g). The suspension was stirred for 0.5 h before filtering the solution into a new flask and removing solvent. The crude product was purified by flash chromatography.

***rac*-5:** R_f = 0.35 (3:1 hexanes:ethyl acetate); yield 73% (10:1 *rac*:*meso* mixture); ^{31}P NMR (121.4 MHz, $CDCl_3$) δ −25.9 (*rac*), −13.1 (*meso*); ^{1}H NMR (300 MHz, $CDCl_3$) δ 0.44 (d, J = 7 Hz, CHC*H*$_3$, 3H), 1.03 (m, CHC*H*$_3$, 9H), 2.44 (o, J = 7 Hz, C*H*CH$_3$, 1H), 3.15 (o, J = 7 Hz, C*H*CH$_3$, 1H), 4.97 (dd, J_{H-P} = 20 Hz, J = 7 Hz, *H*C(P)(N), 1H), 5.35 (dd, J = 7 Hz, J_{H-P} = 2 Hz, *H*C(P)(N), 1H), 7.38 (m, aromatic, 3H), 7.66 (m, aromatic, 2H), 7.85 (m, aromatic, 2H), 8.36 (m, aromatic, 2H), 8.42 (m, aromatic, 2H); ^{13}C NMR (75.4 MHz, $CDCl_3$) δ 18.3 (d, J_{C-P} = 2 Hz), 18.9 (d, J_{C-P} = 10 Hz), 20.0 (d, J_{C-P} = 8 Hz), 20.4 (d, J_{C-P} = 4 Hz), 28.9, 31.3 (d, J_{C-P} = 18 Hz), 66.0 (d, J_{C-P} = 18 Hz), 68.0 (d, J_{C-P} = 31 Hz), peaks at 126−136 ppm were not assigned, 156.9, 157.8; HRMS (*m*/*z*) calcd for $[C_{22}H_{25}N_2O_2P + Na]^+$ 403.1551, found 403.1567.

***rac*-11:** R_f = 0.40 (3:1 hexanes:ethyl acetate); yield 57% of a light yellow oil (25:1 *rac*:*meso* mixture); ^{31}P NMR (121.4 MHz, $CDCl_3$) δ −11.2; ^{1}H NMR (300 MHz, $CDCl_3$) δ 0.97 (d, J = 7 Hz, CHC*H*$_3$, 3H), 0.98 (d, J = 7 Hz, CHC*H*$_3$, 3H), 1.02 (d, J = 7 Hz, CHC*H*$_3$, 3H), 1.25 (m, 7H), 1.60−2.04 (m, 7H), 2.23 (o, J = 7 Hz, C*H*(CH$_3$)$_2$, 1H), 3.52 (o, J = 7 Hz, C*H*(CH$_3$)$_2$, 1H), 4.79 (dd, J_{H-P} = 15 Hz, J = 7 Hz, *H*C(P)(N), 1H), 4.95 (d, J = 7 Hz, *H*C(P)(N), 1H), 7.80 (m, 2H), 8.32 (m, 2H); ^{13}C NMR (75.4 MHz, $CDCl_3$) δ 19.2, 19.3 (d, J_{C-P} = 9 Hz), 20.3 (d, J_{C-P} = 9 Hz), 21.3 (d, J_{C-P} = 12 Hz), 25.9, 27.2, 27.9 (d, J_{C-P} = 19 Hz), 28.5, 29.1 (d, J_{C-P} = 2 Hz), 31.0 (d, J_{C-P} = 16 Hz), 31.8 (d, J_{C-P} = 28 Hz), 33.1 (d, J_{C-P} = 23 Hz), 60.5 (d, J_{C-P} = 23 Hz), 67.7 (d, J_{C-P} = 33 Hz), 127.5, 127.7, 129.4, 130.8, 133.1, 133.2, 156.2, 157.6; HRMS (*m*/*z*) calcd for $[C_{22}H_{31}N_2O_2P + Na]^+$ 409.2021, found 409.2022.

***meso*-11:** R_f = 0.45 (3:1 hexanes:ethyl acetate); yield 21% of a light yellow oil (10:1 *meso*:*rac* mixture); ^{31}P NMR (121.4 MHz, $CDCl_3$) δ −6.8; ^{1}H NMR (300 MHz, $CDCl_3$) δ 1.17 (m, 17H), 1.55−1.75 (m, 6H), 2.30 (m, 2H), 4.75 (d, J_{H-P} = 10 Hz, *H*C(P)(N), 2H), 7.82 (m, 2H), 8.33 (m, 2H); ^{13}C NMR (75.4 MHz, $CDCl_3$) δ 20.5 (d, J_{C-P} = 7 Hz), 21.4 (d, J_{C-P} = 10 Hz), 26.1, 26.4 (d, J_{C-P} = 11 Hz), 29.2 (d, J_{C-P} = 14 Hz), 33.1 (d, J_{C-P} = 17 Hz), 33.5 (d, J_{C-P} = 15 Hz), 65.0 (d, J_{C-P} = 27 Hz), 127.7, 129.5, 133.4, 157.4; HRMS (*m*/*z*) calcd for $[C_{22}H_{31}N_2O_2P + H]^+$ 387.2201, found 387.2092.

General Synthesis of Naphthyldiazaphospholanes (*rac*-8 and *rac*-10). The 1-naphthyl azine (1.55 mmol) in Et_2O (50 mL) was treated with primary phosphine (1.55 mmol) at room temperature. The phthaloyl dichloride (4.65 mmol, 3 equiv) was slowly added and the mixture stirred at room temperature overnight. A portion of 10% aqueous K_2CO_3 (20 mL) was added to the resultant white slurry. Both the organic layer and the aqueous layer were removed via cannula filtration. The solid was washed with water (15 mL) and Et_2O (2 × 15 mL) and the residue dried in vacuo to obtain analytically pure product.

***rac*-8:** yield 42% of an off-white solid; ^{31}P NMR (121.4 MHz, $CDCl_3$) δ −6.4; ^{1}H NMR (300 MHz, $CDCl_3$) δ 6.38 (d, J = 7.3 Hz, 1H), 6.86 (t, J = 7.5 Hz, 1H), 6.96 (m, 2H), 7.02−7.08 (m, 4H), 7.23 (t, J = 7.6 Hz, 1H), 7.39 (t, J = 8.0 Hz), 7.44−7.49 (m, 2H), 7.51 (d, J = 8.0 Hz, 1H), 7.53−7.60 (m, 3H), 7.78 (m, 1H), 7.87 (d, J = 8.6 Hz, 1H), 7.90−7.98 (m, 3H), 8.01 (d, J = 7.9 Hz, 1H), 8.06 (m, 1H), 8.40 (m, 1H), 8.49 (m, 1H); ^{13}C NMR (75.4 MHz, $CDCl_3$) δ 58.8 (d, J_{C-P} = 21 Hz), 62.8 (d, J_{C-P} = 34 Hz), peaks at 120−140 ppm have not been assigned, 157.0, 157.2; HRMS (*m*/*z*) calcd for $[C_{36}H_{25}N_2O_2P + Na]^+$ 571.1551, found 571.1550.

***rac*-10:** yield 61% of a light yellow solid; ^{31}P NMR (121.4 MHz, $CDCl_3$) δ −1.1; ^{1}H NMR (300 MHz, $CDCl_3$: δ 0.0 (m, 1H), 0.7 (m, 2H), 1.1 (m, 1H), 1.24 (m, 2H), 1.5−1.7 (m, 3H), 1.86 (m, 1H), 2.22 (m, 1H), 6.80 (d, J_{H-P} = 14.4 Hz, *H*C(P)(N), 1H), 6.94 (d, J = 7.4 Hz), 7.24 (s, *H*C(P)(N), 1H), 7.30 (d, J = 7.1 Hz, 1H), 7.33 (t, J = 7.7 Hz, 1H), 7.4−7.5 (m, 3H), 7.59 (t, J = 8.1 Hz, 1H), 7.65 (t, J = 7.9 Hz, 1H), 7.75−8.00 (m, 7H), 8.12 (d, J = 8.4 Hz, 1H), 8.42 (m, 2H); ^{13}C NMR (75.4 MHz, $CDCl_3$) δ 26.1, 26.6 (d, J_{C-P} = 16 Hz), 27.3 (d, J_{C-P} = 6), 28.9, 30.8 (d, J_{C-P} = 23 Hz), 33.1 (d, J_{C-P} = 24 Hz), 56.3 (d, J_{C-P} = 25 Hz), 61.9 (d, J_{C-P} = 25 Hz), peaks at 120−135 ppm have not been assigned, 157.3. HRMS (*m*/*z*) calcd for $[C_{22}H_{25}N_2O_2P + Na]^+$ 577.2021, found 577.1998.

(72) Abel, E. W.; Bennett, M. A.; Wilkinson, G. *J. Chem. Soc.* **1959**, 3178−3182.
(73) Herrmann, W. A., Ed. *Synthetic Methods of Organometallic and Inorganic Chemistry*; Thieme: Stuttgart, Germany, 1996.
(74) Giordano, G.; Crabtree, R. H. *Inorg. Synth.* **1990**, *28*, 88−90.
(75) Schrock, R. R.; Osborn, J. A. *J. Am. Chem. Soc.* **1971**, *93*, 3089−3091.
(76) Taylor, R. B.; Jennings, P. W. *Inorg. Chem.* **1981**, *20*, 3997−3999.
(77) Mague, J. T.; Lloyd, C. L. *Organometallics* **1988**, *7*, 983−993.
(78) Orsini, J.; Geiger, W. E. *Organometallics* **1999**, *18*, 1854−1861.
(79) Salo, E. V.; Guan, Z. *Organometallics* **2003**, *22*, 5033−5046.
(80) Rülke, R. E.; Ernsting, J. M.; Spek, A. L.; Elsevier, C. J.; van Leeuwen, P. W. N. M.; Vrieze, K. *Inorg. Chem.* **1993**, *32*, 5769−5778.

***meso*-12.** Cyclohexylphosphine (3 mL, 22.6 mmol) was added to an ether (100 mL) solution of *tert*-butyl azine (3.35 g, 22.6 mmol). HCl (2 M in Et_2O, 11 mL, 22 mmol) was slowly added to this solution, and after a few minutes a solid precipitate formed. Degassed 10% K_2CO_3(aq) (100 mL) was added and the solid dissolved. The ether layer was transferred into a new flask containing anhydrous $MgSO_4$. The solution was filtered from the drying agent into a new flask, at which point phthaloyl dichloride (8 mL, 55.5 mmol, 2.5 equiv) was added, which caused a precipitation of some solid. After the mixture was stirred overnight, degassed 10% K_2CO_3(aq) (100 mL) was added to the reaction mixture and the solid dissolved. The organic layer was transferred via cannula to a new flask containing $MgSO_4$. The aqueous layer was washed with ether (50 mL), and this ether was again transferred to the flask with the $MgSO_4$. The ether solution was filtered into a new flask, where the solvent was removed to give a light yellow solid. Some impurities were removed by washing the solid with hexanes. The solid was dissolved in ethyl acetate and filtered through a short plug (3 in.) of silica gel to give analytically pure product. Yield: 14% (1.312 g, 3.18 mmol) of a light yellow solid. ^{31}P NMR (121.4 MHz, $CDCl_3$): δ −5.9. ^{1}H NMR (300 MHz, $CDCl_3$): δ 0.8−1.4 (m, 6H), 1.25 (d, J_{H-P} = 2 Hz, C(C*H*$_3$)$_3$, 18H), 1.5−1.8 (m, 5H), 4.75 (d, J_{H-P} = 4 Hz, *H*C(P)(N), 2H), 7.78 (m, 2H), 8.26 (m, 2H). ^{13}C NMR (75.4 MHz, $CDCl_3$): δ 26.1, 26.7 (d, J_{C-P} = 10 Hz), 29.3 (d, J_{C-P} = 13 Hz), 30.0 (d, J_{C-P} = 10 Hz), 36.3 (d, J_{C-P} = 17 Hz), 36.8 (d, J_{C-P} = 14 Hz), 68.8 (d, J_{C-P} = 31 Hz), 127.5, 129.8, 133.3, 159.4. HRMS (*m*/*z*): calcd for $[C_{24}H_{35}N_2O_2P + H]^+$, 415.2514; found, 415.2499.

***rac*-16.** Phthaloyl dichloride (6.2 mmol, 4 equiv) was added to a THF (50 mL) solution of bis-phosphine **20** (1.55 mmol) at room temperature. After the mixture was stirred overnight, the solvent was removed in vacuo and the resulting solid was rinsed with 10% K_2CO_3(aq) (20 mL) and ether (2 × 20 mL). ^{31}P NMR (121.4 MHz, $CDCl_3$): δ −4.3. ^{1}H NMR (300 MHz, $CDCl_3$): δ 0.5−2.0 (m, 4H), 5.96 (m, 2H), 6.08 (s, 2H), 6.8−7.4 (m, 16H), 7.83 (m, 4H), 8.32 (m, 4H).

Improved Synthesis of *rac*-17. Diphosphinobenzene (0.32 mL, 2.49 mmol) and phthaloyl dichloride (1.1 mL, 7.72, 3.1 equiv), respectively, were added to a THF (50 mL) solution of phenyl azine (1.088 g, 5.22 mmol, 2.1 equiv). After the mixture was stirred overnight, a white solid precipitated out of solution. The supernatant was removed via cannula filter, and the remaining solid was washed with ether (3 × 30 mL). The remaining solid was dried in vacuo to give a white powder. Yield: 32%. The spectral details of this compound match those previously reported.[12]

General Procedure for Borane Reductions of 3,4-Diazaphospholanes (*rac*-21 and *rac*-22). $BH_3{\cdot}SMe_2$ (2 M in THF, 15 mmol, 15 equiv) was slowly added to a mixture of phosphine (1.0 mmol) in THF (10 mL). After the Schlenk flask was sealed, the mixture was heated to 75 °C overnight. After the solution was cooled to room temperature, the solvent was removed in vacuo and the remaining solid was redissolved in an acetone/water mixture (30:1, 15 mL). Again the Schlenk flask was sealed and heated at 70 °C overnight. The solvent was removed, and the remaining solid was redissolved in EtOAc (30 mL). This mixture was transferred to a separatory funnel, and saturated $NaHCO_3$(aq) (25 mL) was added. The organic layer was removed, and the aqueous layer was washed with EtOAc (20 mL) and CH_2Cl_2 (20 mL). The combined organic layers were dried with $MgSO_4$. The solvent was removed under vacuum, and the products were purified by flash chromatography.

***rac*-21:** R_f = 0.30 (1:1 hexanes:CH_2Cl_2); yield 64% of an off-white solid; ^{31}P NMR (121.4 MHz, $CDCl_3$) δ 16.2; ^{1}H NMR (500 MHz, $CDCl_3$) δ 3.65 (d, J = 14 Hz, CC*H*$_2$N, 1H), 4.18 (d, J = 14 Hz, CC*H*$_2$N, 1H), 4.25 (d, J = 14 Hz, CC*H*$_2$N, 1H), 4.32 (d, J = 14 Hz, CC*H*$_2$N,1H), 4.41 (d, J_{H-P} = 21 Hz, *H*C(P)(N), 1H), 4.65 (d, J_{H-P} = 6 Hz, *H*C(P)(N), 1H), 6.98−7.10 (m, 7H), 7.12−7.22 (m, 4H), 7.23−7.29 (m, 2H), 7.35 (t, J = 8 Hz, 2H), 7.52 (d, J = 8 Hz, 2H), 7.59 (t, J = 8 Hz, 2H); ^{13}C NMR (125.8 MHz, $CDCl_3$) δ 58.0, 59.2, 72.8 (d, J_{C-P} = 17 Hz), 73.4 (d, J_{C-P} = 11 Hz), peaks at 125−142 ppm have not been assigned; HRMS (*m*/*z*) calcd for $[C_{28}H_{25}N_2P + H]^+$ 421.1833, found 421.1823.

***rac*-22:** R_f = 0.70 (1:1 hexanes:CH_2Cl_2); yield 61% of an off-white, glassy solid; ^{31}P NMR (121.4 MHz, $CDCl_3$) δ 11 (bs); ^{1}H NMR (300 MHz, $CDCl_3$) δ −0.11 (bs, 1H), 0.35−2.25 (m, 10H), 3.82 (d, J = 16 Hz, CC*H*$_2$N, 1H), 4.06 (bs, CC*H*$_2$N and *H*C(P)(N), 2H), 4.44 (d, J = 16 Hz, CC*H*$_2$N, 1H), 4.83 (bs, *H*C(P)(N), 1H), 5.20 (d, J = 16 Hz, CC*H*$_2$N, 1H), 6.96 (m, 2H), 7.12 (m, 2H), 7.43−7.67 (m, 7H), 7.73−8.05 (m, 7H), 8.26 (d, J = 9 Hz, 1H), 8.52 (bs, 1H); ^{13}C NMR (75.4 MHz, $CDCl_3$) δ peaks at 24−36 ppm have not been assigned, 59.3 (bs), 59.6 (bs), 68.1 (bs), 68.3 (bs), peaks at 123−138 have not been assigned; HRMS (*m*/*z*) calcd for $[C_{36}H_{35}N_2P + H]^+$ 527.2616, found 527.2604.

General Procedure for Collection of IR Spectra of [*trans*-Rh(PR$_3$)$_2$(CO)Cl] Complexes. A CH_2Cl_2 solution (10 mL) of 3,4-diazaphospholane (0.35 mmol, 4.5 equiv) was cannula-transferred into a CH_2Cl_2 solution (10 mL) of $[Rh(CO)_2Cl]_2$ (0.075 mmol). After it was mixed for 0.5 h, a small amount of the solution was transferred into an NMR tube for ^{31}P NMR (unlocked) analysis. In some cases, a small amount of a fine precipitate formed during the reaction, in which case the reaction mixture was filtered through a Teflon syringe filter (0.45 μm) to remove the solid. The solution was then transferred to a CaF_2 solution cell and the FTIR spectrum taken.

[*trans*-Rh(*rac*-3)$_2$(CO)Cl]: ^{31}P NMR (121.4 MHz, CH_2Cl_2 δ 45.5 (d, J_{P-Rh} = 134 Hz), 46.6 (d, J_{P-Rh} = 135 Hz); FTIR (CaF_2, cm^{-1}) 1990.

[*trans*-Rh(*rac*-5)$_2$(CO)Cl]: ^{31}P NMR (121.4 MHz, CH_2Cl_2) δ 36.8 (d, J_{P-Rh} = 139 Hz); FTIR (CaF_2, cm^{-1}): 1988.

[*trans*-Rh(*rac*-6)$_2$(CO)Cl]: ^{31}P NMR (121.4 MHz, CH_2Cl_2) δ 38.9 (d, J_{P-Rh} = 124 Hz), 40.1 (d, J_{P-Rh} = 125 Hz); FTIR (CaF_2, cm^{-1}): 1994.

[*trans*-Rh(*rac*-7)$_2$(CO)Cl]: ^{31}P NMR (121.4 MHz, CH_2Cl_2) δ 52.7 (d, J_{P-Rh} = 144 Hz); FTIR (CaF_2, cm^{-1}) 2011.

[*trans*-Rh(*rac*-8)$_2$(CO)Cl]: ^{31}P NMR (121.4 MHz, CH_2Cl_2) δ 48.8 (d, J_{P-Rh} = 144 Hz); FTIR (CaF_2, cm^{-1}) 1997.

[*trans*-Rh(*rac*-10)$_2$(CO)Cl]: ^{31}P NMR (121.4 MHz, CH_2Cl_2) δ 58.3 (d, J_{P-Rh} = 139 Hz); FTIR (CaF_2, cm^{-1}) 1980.

[*trans*-Rh(*rac*-11)$_2$(CO)Cl]: ^{31}P NMR (121.4 MHz, CH_2Cl_2) δ 49.1 (d, J_{P-Rh} = 132 Hz), 49.3 (d, J_{P-Rh} = 131 Hz); FTIR (CaF_2, cm^{-1}) 1975.

[*trans*-Rh(*rac*-21)$_2$(CO)Cl] (23). ^{31}P NMR (121.4 MHz, CH_2Cl_2) δ 52.3 (d, J_{P-Rh} = 140 Hz), 54.7 (d, J_{P-Rh} = 138 Hz); FTIR (CaF_2, cm^{-1}) 1982. Crystals suitable for X-ray analysis were grown by layering a CH_2Cl_2 solution of **23** with dry Et_2O.

[*trans*-Rh(*rac*-22)$_2$(CO)Cl]: ^{31}P NMR (121.4 MHz, CH_2Cl_2) δ 55.6 (d, J_{P-Rh} = 127 Hz), 56.4 (d, J_{P-Rh} = 128 Hz); FTIR (CaF_2, cm^{-1}) 1968.

Titration of [Rh(CO)$_2$Cl]$_2$ with *meso*-12. CH_2Cl_2 solutions of $[Rh(CO)_2Cl]_2$ (18.5 mg, 0.0476 mmol, 9.5 mM) and *meso*-**12** (171 mg, 0.414 mmol, 0.083 M) were prepared in a nitrogen-filled glovebag. Aliquots of the phosphine solution were added via syringe to the rhodium solution. After each aliquot, an unlocked ^{31}P NMR and FTIR (CaF_2 solution cell) were taken. ^{31}P NMR (121.4 MHz, CH_2Cl_2): δ −5.8 (s, free phosphine), 38.5 (d, J_{P-Rh} = 130 Hz), 44.9 (d, J_{P-Rh} = 141 Hz). The ^{31}P NMR and FTIR results for each titration are presented in Table 8.

General Synthesis of Rhodium Complexes [Rh(3,4-diazaphospholane)(NBD)Cl] (25 and 26). A CH_2Cl_2 solution (10 mL) of $[Rh(NBD)Cl]_2$ (0.11 mmol) was treated with the 3,4-diazaphospholane (2.2 mmol, 2 equiv) in CH_2Cl_2 (10 mL) at room temperature. The mixture was stirred for 1 h and then put under vacuum to yield a yellow solid, [Rh(NBD)(3,4-diazaphospholane)-

Table 8. Approximate Relative Intensities Observed for ^{31}P NMR Resonances and FTIR Absorptions as a Function of the Total Phosphine to Total Rhodium Ratio

	^{31}P NMR resonance (ppm)			FTIR absorption (cm^{-1})				
P:Rh	−5.8	38.5	44.9	2107	2093[a]	2035	2017	1976
0:1	–	–	–	1	4.5	4.5	0	0
1:1	16	7	1	3.2	15.3	11.5	4.2	1
2:1	10	3	3	–	4.1	2.3	1.9	1
4:1	15	2	3	–	3.3	1	2.5	1.4

[a] This absorption is an overlap of an absorption from $[Rh(CO)_2Cl]_2$ and one from [(*meso*-**12**)Rh(CO)$_2$Cl].

Cl], in quantitive yield (by NMR). Crystals for X-ray crystallography were obtained from CH_2Cl_2 and hexanes at room temperature.

[Rh(*rac*-3)(NBD)Cl] (25): yield 56% of light orange crystals; ^{31}P NMR (121.4 MHz, $CHCl_3$) δ 44.6 (d, J_{Rh-P} = 188 Hz); ^{1}H NMR (300 MHz, $CDCl_3$) δ 1.34 (bs, CC*H*$_2$C, 2H), 3.05 (bs, C═C*H*, 1H), 3.34 (bs,, 1H), 3.50 (bs, C*H*, 1H), 3.60 (bs, C*H*, 1H), 5.09 (bs, C═C*H*, 1H), 5.22 (bs, C═C*H*, 1H), 6.6−6.9 (bs, 2H), 6.89−7.05 (m, 5H), 7.1−7.4 (m, 5H), 7.4−7.6 (m, 3H), 7.7−7.9 (m, 4H), 8.25 (m, 1H), 8.36 (m, 1H). Anal. Calcd for $C_{35}H_{29}ClN_2O_2PRh\cdot0.3CH_2Cl_2$: C, 60.12; H, 4.24; N, 3.98. Found: C, 60.50; H, 4.37; N, 3.95.

[Rh(*rac*-6)(NBD)Cl] (26): yield 75% of light orange crystals; ^{31}P NMR (121.4 MHz, $CHCl_3$) δ 38.3 (d, J_{Rh-P} = 191 Hz); ^{1}H NMR (300 MHz, $CDCl_3$) δ 1.47 (bs, CC*H*$_2$C, 2H), 3.47 (bs, C═C*H*, 1H), 3.67 (bs, C═C*H*, 1H), 3.75 (bs, C*H*, 2H), 5.30 (bs, C═C*H*, 1H), 5.35 (bs, C═C*H*, 1H), 6.13 (dd, J = 2 Hz, 4 Hz, 1H), 6.19 (t, J = 3 Hz, 1H), 6.54 (m, 1H), 6.81 (m, 3H), 6.90 (d, J_{H-P} = 13 Hz, *H*C(P)(N), 1H), 7.31 (m, 2H), 7.41 (m, 1H), 7.59 (m, 3H), 7.79 (m, 2H), 8.23 (m, 1H), 8.35 (m, 1H). Anal. Calcd for $C_{31}H_{25}ClN_2O_4PRh\cdot1.5H_2O$: C, 54.28; H, 4.11; N, 4.08. Found: C, 54.25; H, 4.13; N, 4.11.

Syntheses of [Rh(*rac*-3)$_2$Cl]$_2$ (28). Method A. *rac*-**3** (30 mg, 0.067 mmol, 2 equiv) and Rh(*rac*-**3**)(NBD)Cl (20 mg, 0.029 mmol) were mixed in dry CH_2Cl_2 (10 mL). AgOTf (7.6 mg, 0.029 mmol, 1 equiv) in CH_2Cl_2 (10 mL) was added to the phosphine mixture. Although it is not necessary, the reaction can be accelerated by bubbling H_2 gas through the reaction mixture, which immediately turns the solution dark red. After it was stirred overnight, the reaction mixture was filtered through Celite, and the volatiles were removed under vacuum to yield a deep red solid. Recrystallization from CH_2Cl_2 and hexanes gave X-ray-quality crystals. Yield: 44% (158 mg, 0.074 mmol) of red-orange solid. ^{31}P NMR (121.4 MHz, $CHCl_3$): δ 58.2 (d, J_{Rh-P} = 215 Hz). ^{1}H NMR (300 MHz, $CDCl_3$): δ 5.78 (d, J = 8 Hz, 4H), 6.18 (m, 8H), 6.28 (s, 4H), 6.57 (m, 4H), 6.80 (m, 4H), 6.88 (t, J = 8 Hz, 4H), 7.05 (m, 8H), 7.18 (m, 8H), 7.32 (m, 4H), 7.49 (m, 12H), 7.74 (m, 8H), 7.90 (m, 4H), 8.14 (m, 4H), 8.17 (m, 4H), 8.2 (m, 4H). Anal. Calcd for $C_{112}H_{84}Cl_2N_8O_8P_4Rh_2\cdot3H_2O\cdot2CH_2Cl_2$: C, 59.67; H, 4.13; N, 4.88. Found: C, 59.1; H, 4.13; N, 4.90.

Method B. A solution of *rac*-**3** (40 mg, 0.089 mmol, 2 equiv) in CH_2Cl_2 (10 mL) was added to a CH_2Cl_2 (10 mL) solution of $[Rh(COD)_2]BF_4$ (18 mg, 0.045 mmol). Over the course of 1 h, the solution turns from dark red-brown to a lighter red-orange. Again, the reaction can be accelerated by bubbling H_2 through the reaction mixture, which causes an immediate color change to dark red. The reaction mixture was filtered through Celite, and the volatiles were removed under vacuum to yield a deep red solid. The spectroscopic characteristics of this compound are identical with those described above.

Syntheses of [Rh(*rac*-17)Cl]$_2$ (32). Method A. The bisphosphine *rac*-**17** (66 mg, 0.081 mmol, 2 equiv) and [Rh(COD)Cl]$_2$ (20 mg, 0.041 mmol) were dissolved in CH_2Cl_2 (10 mL), and the mixture was stirred for 3 h. The solvent was removed under vacuum, and the remaining orange-red solid was recrystallized from CH_2Cl_2 with hexanes to give X-ray-quality crystals. Yield: 76% of orange-red solid. ^{31}P NMR (121.4 MHz, $CHCl_3$): δ 87.7 (d, J_{P-Rh} = 209 Hz). ^{1}H NMR (300 MHz, $CDCl_3$): δ 5.68 (s, 4H), 6.13 (s, 4H), 7.08−7.28 (m, 28H), 7.45 (m, 12H), 7.85 (m, 8H), 8.30 (m, 4H), 8.37 (m, 4H). Anal. Calcd for $C_{100}H_{72}Cl_2N_8O_8P_4Rh_2\cdot2H_2O\cdot C_6H_{14}$: C, 62.51; H, 4.45; N, 5.50. Found: C, 62.25; H, 4.55; N, 5.50.

Method B. A solution of *rac*-**17** (40.9 mg, 0.050 mmol) in CH_2Cl_2 (10 mL) was added to a solution of $[Rh(COD)_2]BF_4$ (19.9 mg, 0.049 mmol) in CH_2Cl_2 (10 mL). The solution color changes from dark red to a lighter red-orange. After 1 h of stirring at room temperature, the solvent could be removed under vacuum to give a product, which is presumably the cationic complex [Rh(COD)(*rac*-**17**)]BF_4 by NMR. ^{31}P NMR (121.4 MHz, $CHCl_3$): δ 56.6 (d, J_{P-Rh} = 166 Hz). ^{1}H NMR (300 MHz, $CDCl_3$): δ 1.5−2.7 (m, 8H), 5.78 (d, J = 8 Hz, 4H,), 6.18 (bs, 8H), 6.28 (s, 4H), 6.57 (m, 4H), 6.80 (m, 4H), 6.88 (t, J = 8 Hz, 4H), 7.05 (m, 8H), 7.18 (m, 8H), 7.32 (m, 4H), 7.49 (m, 12H), 7.74 (m, 8H), 7.90 (m 4H), 8.14 (m, 4H), 8.17 (m, 4H), 8.2 (m, 4H). Upon recrystallization of this complex from CH_2Cl_2 with hexanes, crystals with spectroscopic characteristics the same as those described above for **33** were isolated.

[Pd(*rac*-15)(allyl)Cl] (33). A CH_2Cl_2 solution (10 mL) of $[Pd(allyl)Cl]_2$ (0.11 mmol) was treated with a solution of *rac*-**15** (2.2 mmol, 2 equiv) in CH_2Cl_2 (10 mL) at room temperature. The mixture was stirred for 1 h and then put under vacuum to yield a yellow-green solid. Crystals for X-ray crystallography were obtained from CH_2Cl_2 and hexanes at room temperature. Yield: 33% of yellow-green crystals. ^{31}P NMR (121.4 MHz, $CHCl_3$): δ 72.1, 70.6. ^{1}H NMR (300 MHz, $CDCl_3$): δ 2.41 (m, 8H), 3.24 (bs, 1H), 4.68 (bs, 1H), 5.45 (m, 1H), 6.19 (d, J = 9 Hz, 1H), 6.33 (d, 5 Hz, 1H), 6.45 (bs, 1H), 6.6 (bs, 1H), 6.90 (t, 8 Hz, 1 H), 6.93 (bs, 1H), 7.0−7.3 (m, 8H). Anal. Calcd for $C_{27}H_{28}ClN_2O_4PPd$: C, 52.52; H, 4.57; N, 4.54. Found: C, 52.79; H, 4.55; N, 4.52.

Ring-Opening Transformation of 34 to 35. A gray CH_2Cl_2 solution (10 mL) of [(COD)Pd(Me)Cl] (26.7 mg, 0.101 mmol) was treated with a solution of *rac*-**17** (79 mg, 0.096 mmol) in CH_2Cl_2 (10 mL) at room temperature. After it was stirred overnight, the solution was light yellow with some gray solid. The solution was filtered through Celite and the solvent removed to yield a yellow solid (**34**). ^{31}P NMR (121.4 MHz, $CHCl_3$): δ 42.8 (d, J_{P-P} = 31 Hz), 64.7 (d, J_{P-P} = 31 Hz). ^{1}H NMR (300 MHz, $CDCl_3$): δ 0.47 (dd, 3H, J_{H-P} = 8.8, 2.6 Hz, CH_3); the presence of unreacted *rac*-**17** precluded interpretation of the remaining signals. Recrystallization of this compound from CH_2Cl_2/hexanes yielded X-ray-quality crystals of **35**. Yield: 79% of pale yellow crystals. ^{31}P NMR (121.4 MHz, $CHCl_3$): δ 48.3 (d, J_{P-P} = 27 Hz), 56.3 (d, J_{P-P} = 27 Hz). ^{1}H NMR (300 MHz, $CDCl_3$): δ 1.46 (d, J_{H-P} = 11.0 Hz, C*H*$_3$, 3H), 5.83 (d, J_{H-P} = 8.2 Hz, 1H), 6.26 (dd, J = 11.3, 1.4 Hz, 1H), 6.61 (m, 1H), 6.74 (d, 6.1 Hz, 1H), 7.0−7.28 (m, 17H), 7.36 (m, 5H), 7.55 (m, 3H), 7.7 (m, 1H), 7.78 (m, 1H), 7.92 (m, 2H), 8.02 (m, 1H), 8.37 (m, 1H), 8.43 (m, 1H). The final product contains about 14% [(*rac*-**17**)$PdCl_2$] (**36**). Anal. Calcd for $C_{25}H_{19}ClN_2O_2P_2Pd\cdot0.14C_{24}H_{16}Cl_2N_2O_2P_2Pd\cdot0.5H_2O\cdot0.5CH_2Cl_2$: C, 60.23; H, 3.98; N, 5.48. Found: C, 60.10; H, 3.95; N, 5.60.

Preparation of [(*rac*-17)PdCl$_2$] (36). A CH_2Cl_2 (10 mL) solution of *rac*-**17** (116 mg, 0.142 mmol) was cannulated into a CH_2Cl_2 (10 mL) solution of [(COD)$PdCl_2$] (40 mg, 0.14 mmol). After it was stirred for 2 h, the resulting mixture was diluted with hexanes, which resulted in precipitation of an off-white solid. The solid was isolated by filtration and dried under vacuum. Yield: 85% (118.6 mg, 0.119 mmol) of an off-white solid. ^{31}P NMR (121.4 MHz,

$CHCl_3$): δ 76.0. ^{1}H NMR (300 MHz, $CDCl_3$): δ 6.19 (d, $J = 7$ Hz, (P)(N)C-*H*, 2H), 7.08 (m, 8H), 7.23 (m, 6H), 7.41 (m, 10H), 7.52 (m, 2H), 7.93 (m, 4H), 8.34 (m, 2H), 8.42 (m, 2H).

Acknowledgment. The Department of Energy and Dow Chemical Co. provided support for this work. We thank Dr. Ilia Guzei for his crystallographic work and expertise and for assistance with the program Solid-G. We thank Dr. Thomas Clark for valuable advice and some phosphine samples.

Supporting Information Available: Crystallographic data for **23**, **25**, **26**, **28**, **30**, **32**, **33**, and **35** as CIF files. This material is available free of charge via the Internet at http://pubs.acs.org.

OM050922G